THE HAND1 LINEAGE REVEALS DISTINCT ROLES FOR HAND FACTORS DURING CARDIOVASCULAR DEVELOPMENT

Ralston M. Barnes

Submitted to the faculty of the University Graduate School
in partial fulfillment of the requirements
for the degree
Doctor of Philosophy
in the Department of Anatomy & Cell Biology,
Indiana University

October 2010

Accepted by the Faculty of Indiana University, in partial
fulfillment of the requirements for the degree of Doctor of Philosophy.

_____
Anthony B. Firulli, Ph.D., Chair

_____
Joseph P. Bidwell Ph.D.

Doctoral Committee

_____
Simon J. Conway Ph.D.

September 2, 2010

_____
Loren J. Field Ph.D.

DEDICATION

“To My Mother & Father, for the continued love, support, & above all respect.

To Emily, Josh, Jason, Lesley & Taylor, for the many smiles, adventures, & endless joy you bring to the due process of life.

To my brother, may you always find tigers in your pockets and continue to ride elephants into battle.”

ABSTRACT

Ralston M. Barnes

THE HAND1 LINEAGE REVEALS DISTINCT ROLES FOR HAND FACTORS DURING CARDIOVASCULAR DEVELOPMENT

The basic Helix-Loop-Helix (bHLH) transcription factors Hand1 and Hand2 play critical roles in the development of multiple organ systems during embryogenesis. The dynamic expression patterns of these two factors within developing tissues obfuscates their respective unique and redundant organogenic functions. To define cell lineages potentially dependent upon *Hand* gene expression, we generated a mutant allele in which the coding region of *Hand1* is replaced by *Cre* recombinase. Subsequent Cre-mediated activation of *β-galactosidase* or *eYFP* reporter alleles enabled lineage trace analyses that clearly define the fate of *Hand1*-expressing cells. Comparisons between *Hand1* expression and *Hand1*-lineage greatly refine our understanding of its dynamic spatio-temporal expression domains and raise the possibility of novel Hand1 functions in structures not thought to be Hand1-dependent. To genetically examine functional overlap between *Hand1* and *Hand2*, we conditionally deleted *Hand2* from *Hand1*-expressing cells. *Hand2* conditional knockout mice die midgestation and exhibit cardiovascular and limb defects. Moreover, *Hand2* lineage-restricted deletion from the proepicardial organ results in defective epicardialization and failure to form coronary arteries. Together, these novel data demonstrate a hierarchal relationship whereby transient *Hand1* expression within

the septum transversum defines epicardial precursors that depend upon subsequent Hand2 function.

Anthony B. Firulli, Ph.D., Chair

TABLE OF CONTENTS

Chapter One

Introduction……1

Hand1 Lineage Analysis...……32

Chapter Two

Hand2 Deletion in the Hand1 Lineage……42

Chapter Three

Discussion…….. 52

Overview & Future Aims……62

Figures ……66

Chapter Four

Methods……..87

References……..94

Curriculum Vitae

Chapter One

Introduction

Overview of heart development

The heart originates from a population of bilaterally symmetrical mesodermal cells located within the anterior of the early headfold-stage embryo. This population of cells, termed the cardiac crescent, is characterized by the expression of a restricted profile of transcription factors, including the homeodomain transcription factor Nkx2.5 and the T-box containing transcription factor Tbx5 (Olson, 2002). The limbs of the cardiac crescent ultimately migrate to fuse along the ventral midline, forming a linear tube comprised of myocardial and endocardial layers intervened by extracellular matrix termed the cardiac jelly. This tube is then patterned along an anterior-posterior axis and divided into a series of segments, distinguishable through their unique transcriptional profiles, which will give rise to the conotruncus, the right and left ventricles, the atrioventricular (AV) canal, and the left and right atria. As the heart tube lengthens, it loops to the right displacing its ventral surface, termed the outer curvature, laterally. As the primitive cardiac chambers mature, a subpopulation of endocardial cells residing within the AV canal, undergo epithelial-to-mesenchymal transition (Kreuger et al., 2005), delaminating and invading the cardiac jelly to form structures known as the AV cushions (Eisenberg and Markwald, 1995). The mesenchymal cells of the AV cushions subsequently

differentiate into the fibrous tissue, which is remodeled to form the AV valves (Armstrong and Bischoff, 2004). Roughly concurrent with AV cushion formation, neural crest-derived ectomesenchyme populating the pharyngeal arches dorsal to the conotruncus differentiates into smooth muscle cells that subsequently organize into bilaterally symmetrical blood vessels termed the pharyngeal arch arteries. These vessels are ultimately remodeled to form the great arteries of the aortic arch, the vasculature through which blood exits the heart (Hiruma et al., 2002).

Recent work has defined two major fields of cardiac progenitors, dubbed the first (FHF) and second heart fields (SHF) (Cai et al., 2003). The FHF has been defined as the region of splanchnic lateral plate mesoderm that contributes to descendents of the left ventricle, atria, and inflow region while the SHF is derived from pharyngeal mesoderm cells which contribute to the right ventricle, OFT, and atria in a mixed population with the FHF (Cai et al., 2003; Kelly, 2005). Experiments in which mice lacking *Islet-1* failed to extend the primitive heart tube confirmed that cells of the SHF are cardiogenic progenitors that contribute to heart development prior to neural crest contributions to the aorticopulmonary cushions and the smooth musculature of the OFT and aortic arch. Lineage-tracing experiments using an *Islet-1*^{Cre} show that the SHF gives rise to cardiomyocytes of the OFT, right ventricle, atria, and inflow region segments of the heart (Cai et al., 2003; Yuan et al., 2000).

Overview of bHLH Proteins

Heart fields are first specified at E7.5 when cytokines from the transforming growth factor beta and Fibroblast Growth Factor superfamilies induce cardiogenesis (Abu-Issa and Kirby, 2007). The cardiac differentiation program is mediated by transcription factors via a positive feed-forward mechanism (Bruneau, 2002; Takeuchi and Bruneau, 2009). Numerous transcription factors drive cardiac specification, differentiation, and morphogenesis including, members of the *Nkx2*, *Gata*, *Mef2*, *Srf*, *Tbx*, *Irx*, and *Twist* families (Barnes and Firulli, 2009; Firulli and Thattaliyath, 2002; Kirby, 2007; Takeuchi and Bruneau, 2009).

The *Twist* family of basic helix-loop-helix (bHLH) group of transcription factors exerts a determinative influence on a variety of developmental pathways, notably cardiac development. These transcription factors are characterized by a highly evolutionary conserved bHLH domain that mediates DNA binding and dimerization (Massari and Murre, 2000). More specifically, this motif contains an N-terminal α-helix with 20 basic residues that interact with DNA at the canonical DNA sequence “CANNTG” (known as an E-box), a middle loop region, and a C-terminal amphipathic α-helix. bHLH proteins are generally categorized into two main classes, class A factors, which are represented by the near-ubiquitously expressed E-proteins (E12, E47, HEB, ITF), and class B factors, which are expressed in a tissue-restricted manner (Firulli, 2003). Dimers differ in their

affinity for DNA and in their ability to activate transcription from E-box-containing promoters.

Brief Overviews of Hand Factors during Heart Development

Hand1 and Hand2 Twist-family member bHLH transcription factors serve an important role during embryogenesis and have demonstrated a critical role for the *Hand* genes during cardiac morphogenesis (Firulli, 2003). During mouse cardiogenesis, *Hand2* and *Hand1* are expressed in a complementary fashion in the future right and left ventricles, respectively (Firulli, 2003). Targeted deletion of the *Hand2* gene in mice demonstrated a requirement for *Hand2* in the development of cells fated to form the future right ventricle during the period of cardiac looping (Srivastava et al., 1997). *Hand2* null mice die between E9.5–10.5, exhibit hypoplastic first and second arches, secondary to apoptosis, and the third and fourth arches fail to form (Srivastava et al., 1997; Thomas et al., 1998). Mice lacking the *Hand1* gene die between E8.5 and E9.5 due to deficiencies in the extra embryonic mesoderm thereby precluding detailed analysis of its role in cardiogenesis (Firulli et al., 1998). Embryos homozygous for a *Hand1* cardiac-specific conditional allele displayed defects in the left ventricle, endocardial cushions, and exhibited dysregulated ventricular gene expression (McFadden et al., 2005). No right ventricular phenotypes are evident. Intercross of the cardiac-specific *Hand1* mutant mouse into the *Hand2* systemic null allele shows the importance of *Hand* gene dosage for proper heart development. These mice display both left and right ventricle hypoplasia. Interestingly, this

genetic interaction is difficult to explain, as *Hand1* is never detected within the right ventricle, an AH-derived structure. This suggests that either *Hand1* is expressed at low levels early in the specification of right ventricular cardiomyocytes or that signaling networks hobbled by *Hand1* loss-of-function are sensitive to *Hand2* haploinsufficiency.

Hand1 is required for proper cardiac morphogenesis and is essential for extra-embryonic and trophoblast-cell differentiation

Hand1 was cloned from a yeast-2-hybrid screen using an E12 bait (Cserjesi et al., 1995). *Hand1* shares the highest degree of sequence identity with *Hand2* and to a lesser extent with Twist1 and other bHLH family members (Srivastava et al., 1995). *In Situ* hybridization shows *Hand1* is expressed within the trophoblast cells of the ectoplacental cone prior to E7.5 with expression throughout the yolk sac, chorion & extra embryonic mesoderm (Cserjesi et al., 1995). Extra-embryonic expression of *Hand1* is maintained throughout later stages of embryonic development (Cserjesi et al., 1995).

In the embryo, *Hand1* expression is first observed at embryonic day E7.5 in the lateral plate mesoderm that contributes to form the primitive heart tube (Srivastava et al., 1997). At E8.5 *Hand1* is detected in the developing heart tube, pericardium, & the distal regions of lateral mesoderm (Biben and Harvey, 1997, Cserjesi et al., 1995, Srivastava et al., 1995). During rightward looping of the heart, *Hand1* becomes restricted to the outer curvature of the myocardium

contributing to the presumptive left ventricle, the septum transversum, and the pericardium where it persists thru E13.5 (Cserjesi et al., 1995, Firulli et al., 1998, Thomas et al., 1998). *Hand1* expression continues to accumulate throughout the lateral mesoderm where it persists in the developing gut distal to the duodenum (Morikawa and Cserjesi, 2004). *Hand1* is also expressed throughout the umbilical and vitelline vein/artery by E9.5 (Firulli et al., 1998). *Hand1* is also detected in the distal portions of the limb. At E11.5 it is expressed in the antero-ventral domain of the limb bud where it is maintained thru E13.5 (Fernandez-Teran et al., 2003). *Hand1* is expressed in adult-rodent and human hearts as well, where they are thought to play a role in preventing hypertrophy.

Hand1 is also expressed within the cranial and cardiac neural crest cells occupying the medial pharyngeal arches and first appears at E9.5 as they begin to populate the outflow tract where they contribute to the smooth muscle lining the pulmonary artery (Cserjesi et al., 1995, Barbosa et al., 2007, Vincentz et al., 2008). *Hand1* continues to accumulate in structures derived from neural crest cells where by E10.5 it is detected in the sympathetic and splanchnic ganglia of the peripheral nervous system and the first and second aortic arch (Cserjesi et al., 1995, Firulli et al., 1998, Howard et al., 1999, Morikawa and Cserjesi, 2004). At E12.5, *Hand1* is expressed in the sypatho/adrenal lineage as well as the mandible, which is derived from the pharyngeal arches (Cserjesi et al., 1995, Firulli et al., 1998, Morikawa and Cserjesi, 2004). *Hand1 mRNA* continues to

persist in rudiments of neural crest derived tissues until E14.5 (Cserjesi et al., 1995, Morikawa and Cserjesi, 2004).

Heart development of *Hand1*-null mutants is arrested during formation of the heart tube where the caudal portion failed to fuse as shown by marker analysis (Firulli et al., 1998). Analysis of homozygous *Hand1*-null embryos shows that early myocardial markers such as *Nkx2.5*, *Mef2C*, *Gata4*, and *Mlc2a* were unaffected (Firulli et al., 1998, Riley et al., 1998). *Hand1*-null embryoid bodies are capable of differentiating into cardiomyocytes (Riley et al., 2000) indicating that heart defects are not due to a failure of the myocardium to differentiate but due to improper patterning of the heart (Firulli et al., 1998). Tetraploid experiments using *Rosa26* derived; *Hand1*-null ES cells are underrepresented in the left ventricular chamber but are capable of differentiating into cardiomyocytes *in vitro* indicating that *Hand1* is not necessarily essential for cardiomyocyte differentiation but is required for proper patterning of the left ventricle (Riley et al., 2000). Furthermore, the reduction of the left ventricle in mice with a conditional ablation of *Hand1* in the heart substantiate this conclusion (McFadden et al., 2005), though more detailed analysis pairing the conditional *Hand1*-allele with a wider range of available Cre lines would be useful to support these findings.

Hand1 is restricted to the outer wall of the left ventricular chamber during rightward looping of the heart. An asymmetric expansion of cells in this outer curvature is tightly intertwined in the process, implicating a role for *Hand1* in

proliferation during heart remodeling. Misexpression of *Hand1* in the myocardium of both ventricular chambers resulted in an expansion of the outer curvature of both the left and the right ventricle (Togi et al., 2004). Over expression of *Hand1* specifically in *Hand1* expressing cells resulted in abnormal looping (Risebro et al., 2006). Though these hearts were accompanied by a failure of ventricular expansion, thorough analysis revealed that *Hand1* over-expression resulted in left-ventricular defects due to elevated myocyte density and reduced myocardial differentiation. Furthermore, cells over expressing *Hand1* in *Hand1*-positive neural crest cells resulted in an elongated outflow tract due to continued proliferation and a failure to commit to differentiation (Risebro et al., 2006). The complimentarity of the phenotype between loss-of-function and gain-of-function mutations of *Hand1* suggest a conserved role for *Hand1* during heart morphogenesis. Additionally, they support the hypothesis that proper *Hand* gene dosage is essential for proper development, which has been elucidated in further studies with *Hand2* (Barbosa et al., 2007, McFadden et al., 2005).

Further analysis of *Hand1* null mice clearly shows that *Hand1* is essential for the development of extra-embryonic tissue. *Hand1* is expressed in all subtypes of trophoblast giant cells within the ectoplacental cone and chorion (Simmons et al., 2008, Vasicek et al., 2003). *Hand1*-null embryos exhibit a dramatic downregulation of *placental lactogen 1 (Pl1)* within the ectoplacental cone. *Pl1 codes for* a hormone required for embryonic viability and placental homeostasis and is expressed within the developing giant-trophoblast cells

(Cross et al., 2002, Firulli et al., 1998, Hughes et al., 2004). *Pl1* was detected in only a subset of giant cells outside of the ectoplacental cone in the placenta of *Hand1*-null embryos (Riley et al., 1998). The ectoplacental cone only contains an increased number of giant cell precursors, suggesting Hand1 plays a role during giant cell differentiation (Gardner et al., 1973). This conclusion gains support when considering that over-expression of *Hand1* leads to an increase of *Pl1* in giant cells (Cross et al., 1995) and *Hand1* homozygous mutant trophoblast cells display deficiencies in differentiation and normal invasive behavior (Hemberger et al., 2004), illustrating the critical role for *Hand1* in trophoblast cell development. Furthermore *Hand1* hypomorphic alleles, which extend embryonic viability up to E12.5 exhibit an intermediate level of *Pl1* expression when compared to wildtype and Hand1 null embryos (Firulli et al., 2010).

In regard to extra-embryonic tissues, Hand1 is also required for the formation of the extra-embryonic membrane, where it is expressed within the mesodermal compartment. *Hand1*-null embryos exhibit abnormalities of the extra-embryonic vasculature following formation of the yolk sac by E7.5 (Firulli et al., 1998, Morikawa and Cserjesi, 2004). Analysis of *Hand1*-null embryos shows that the yolk sac maintains an immature vascular plexus and smooth muscle cells required for blood vessel support during vasculogenesis failed to undergo normal recruitment (Morikawa and Cserjesi, 2004). Collectively the trophoblast and extra embryonic vascular phenotypes are the likely cause of embryonic death as the observed phenotypes within neural crest and cardiac cell

populations would not result in embryonic lethality until later gestation or even after birth.

Mechanistically Hand1 was initially thought to interact only with ubiquitously expressed E-proteins (Massari and Murre, 2000). Mammalian two-hybrid and pull-down assays confirmed however, that Hand1 could form homodimers as well as interact with other tissue restricted bHLH proteins, such as Hand2 (Firulli et al., 2000) and later Twist1 (Firulli 2005). Similar to Twist1, Hand1 was shown via EMSA's to inhibit MyoD/E12 DNA-binding presumably by directly competing for E-protein and MyoD dimers (Firulli et al., 2000). Although the biological relevance of this observation is moot given Hand1 and MyoD are not co-expressed during development, it does speak to the evolutionary conservation within the Twist-family and their ability to alter the bHLH dimer pool within a cell simply by reorganizing the dimer partner complexes by regulating their dimer choices. The idea of dimer regulation as a mechanism to control biological developmental programs was then postulated and the evidence of such regulation was then sought.

Dimer partner choice must infer dimer regulation on Twist family proteins and this was first demonstrated with Hand1. The LIM domain protein FHL2 is capable of interacting with Hand1 in the nucleus and repressing function of Hand1/E12 heterodimers though it is incapable of effecting Hand1/Hand1 homodimer activity (Hill and Riley, 2004). Additionally, gain-of-function expression of a DNA-binding mutant Hand1 protein does not inhibit Hand1's

ability to induce limb polydactyly suggesting that alteration of the bHLH dimer pool is more influential on biological program then direct cis-acting targets for functional Hand1 transcriptional complexes (McFadden et al., 2002). Indeed when considering these results carefully, the most plausible mechanism to explain these findings would be that Hand1 dimerization acts as a dominant negative factor antagonizing the equilibrium of the bHLH dimer pool. Support of this model is observed in gain-of-function experiments that show expression of a Hand1 proline mutant, which disrupts the HLH domain does not result in polydactyly (McFadden et al., 2002)

If altering the overall expression level of Twist-family proteins can alter the bHLH dimer pool within the cell when expression levels are within normal levels, are there additional mechanisms that control dimer choice? Indeed post-translational modification of Twist proteins influences dimer complex formation: Hand1 phosphoregulation at Serine 107 and Threonine 109 modulates dimer partner specificity. Protein Kinase A and C (PKA and PKC) which can phosphorylate these Hand1 residues while b56d-containing Protein Phosphatase 2A (PP2A) can specifically dephosphorylate these residues (Firulli et al., 2003). Phosphorylation of Hand1 increases during differentiation of trophoblast giant-cells and this is associated with a downregulation of b56d (Firulli et al., 2003). Recently, it has been shown in trophoblast giant-cells that Hand1 is negatively regulated by interacting with I-mfa, which sequesters it to the nucleolus (Martindill and Riley, 2008, Martindill et al., 2007). Interestingly, the Hand1

hypophosphorylation mutant targets directly to the nucleolus where the protein is sequestered, preventing differentiation (Martindill and Riley, 2008, Martindill et al., 2007). Conversely a Hand1 phosphorylation mimic resides solely within the nucleus and expression drives trophoblast differentiation (Martindill and Riley, 2008, Martindill et al., 2007). This data demonstrates that phosphoregulation modulates dimer choice in at least two ways. First by directly effecting protein affinity and second my dictating cell localization.

To date, upstream regulators and downstream transcriptional targets of *Hand1* have been difficult to ascertain. Hand1 *in vitro* can activate the promoter of cardiac *atrial natriuretic factor*, implicating it as a potential target of *Hand1* (Morin et al., 2005). *Hand1* is coexpressed in the heart with *Thymosin b4*, which is downregulated in Hand1-null embryoid bodies, as well as *cytostatin C*, and *aCA*, which are found to be upregulated (Smart et al., 2002). Ectopic expression of *Tbx5* results in enhanced *Hand1* expression while simultaneously suppressing *Hand2,* suggesting that *Tbx5* can impart left ventricular identity upon *Hand1* expressing cells found throughout this region (Takeuchi et al., 2003). Regarding upstream regulation, *Nkx2.5* knock-out mice, which regulates expression of a number of cardiac specific genes, results in a severe reduction of *Hand1* in the heart, implicating that *Nkx2.5* may be upstream of *Hand1* (Tanaka *et al.*, 1999).

Hand2 is Required During Development of the Heart, Limbs, Autonomic Nervous System, & Other Neural Crest Derived Structures

Hand2 was identified in a low stringency cDNA library screen using a *Hand1* bHLH domain probe (Srivastava et al., 1995). In the chick, *Hand2* is first detected in the lateral mesoderm, and cardiac crescent; later it is expressed throughout the developing heart tube (Srivastava et al., 1995). In the mouse, *Hand2* is first expressed at E7.5 in the maternally derived decidua and is first detected in the embryo at E7.75 in the lateral mesoderm that forms the cardiac crescent and is maintained throughout the linear heart tube to E8.0 (Srivastava et al., 1997). At the onset of cardiac looping, *Hand2* cardiac expression subsequently restricts to the forming right ventricle and outflow tract downregulating within the left ventricle, which expresses *Hand1* (Firulli et al., 1998, McFadden et al., 2000, Overbeek, 1997, Srivastava et al., 1997). *Hand2* is also expressed in the pharyngeal arches and neural crest cells where they give rise to craniofacial structures, outflow tract, the sympathetic nervous system, extra-adrenal chromaffin cells, as well as the posterior portion of the limb buds, (Charite et al., 2000, Gestblom et al., 1999, Ruest et al., 2003).

Hand2-null embryos die by E9.5 suffering with severe morphological deficiencies in the heart as they have only a single left ventricle (Srivastava et al., 1997). *Hand2*-null embryos undergo apoptosis in the region of the forming right ventricle (bulbous cortis) and results in a down regulation of ventricular markers such as *Irx4*, suggesting a role for maintenance of the right ventricle progenitors

and supporting ventricular expansion (Bruneau et al., 2000, McFadden et al., 2000, Yamagishi et al., 2001). This role for *Hand2* is further supported by evidence that a conditional deletion of *Gata4* in the heart, which has been shown to directly regulate a ventricular enhancer element of *Hand2*, results in right ventricular hypoplasia (McFadden et al., 2000, Zeisberg et al., 2005). Overexpression of *Hand2* in the ventricles results in outward expansion of the ventricular chamber as well as an absence of the interventricular septum, which is replaced by an expanded trabecular domain, further establishing a role for *Hand2* in supporting ventriculogenesis (Togi et al., 2006). In mice that have a homozygous-null allele for *m-Bop*, the histone deacetylase-dependent transcriptional repressor, *Hand2* expression is down regulated and there is an associated disruption of ventricular myocardial development (Gottlieb et al., 2002). Data that may partially explain the *Hand* sided expression can be seen in studies of Tbx5 (Takeuchi et al., 2003). Tbx5 can suppress *Hand2* concurrent with upregulation of *Hand1*.

Hand2 has been shown to directly regulate the *Nppc* gene which codes of atrial naturetic factor (Anf*).* In *Hand2*-null mice, *Anf* is downregulated while a *Hand2*-heterodimer has been shown to *trans*-activates the *Anf* promoter (Thattaliyath et al., 2002a). Additionally, *Hand2* cooperates with *Mef2c* to activate both *Anf* and *aMHC* (Zang et al., 2004a, Zang et al., 2004b). Moreover, Hand2 can synergize with Gata4 to activate *Anf* as well, revealing a multifunctional role for *Hand2* in *Anf* regulation (Dai et al., 2002).

Recently, it has been demonstrated that *Hand2* is a direct target of microRNAs. A heart conditional knock out of *Dicer*, an enzyme required for processing of precursor microRNAs, results in the upregulation of *Hand2* (Zhao et al., 2007). miR-*1*, a cardiac and skeletal muscle-restricted microRNA, is negatively affected in the *Dicer* knockouts. miR-1 over expression leads to a reduction in ventricular myocardium and is also capable of directly targeting *Hand2* (Zhao et al., 2005).

Hand2 is also expressed throughout the cephalic neural crest mesenchyme of the first and second pharyngeal arches and plays a role in facial morphogenesis, where expression is directed by a *Hand2* enhancer element complete and separate from the ventricular heart enhancer (McFadden et al., 2000, Ruest et al., 2003, Yanagisawa et al., 2003). *Endothelin-1* (*Edn1)*, which is expressed in the epithelial layer of the branchial arches, regulates *Hand2* and is downregulated in the branchial arches in *Edn1*-null mice (Ivey et al., 2003, Li and Li, 2006, Thomas et al., 1998a). The *Edn1* downstream effectors *Dlx5* & *Dlx6* directly regulate *Hand2* transcription via a Dlx cis-element located within the Hand2 branchial arch enhancer (Charite et al., 2001, Fukuhara et al., 2004). Targeted deletion of the *Hand2* branchial arch enhancer confirms that *Hand2* is required for craniofacial development as mutants exhibit craniofacial abnormalities that include cleft palate, mandibular hypoplasia, as well as a range of cartilage malformations (Yanagisawa et al., 2003). A small domain of *Hand2* expressing cells in the distal most portion of the pharyngeal arches appears to be

Edn1 independent and is instead thought to be regulated by GATA3 (Ruest et al., 2004). A conditional neural crest cell deletion of *Mef2c* shows that *Mef2c* likely mediates Endothelin signaling in the pharyngeal arches and is required for *Dlx 5 & 6* and *Hand2* (Verzi et al., 2007). Pharyngeal arch mesenchyme undergoes apoptosis in *Hand2*-null embryos by *E9.5*; however cell death is partially rescued when mice are also null for *Apaf1* (Aiyer et al., 2005, Thomas et al., 1998a).

Hand2 is necessary for limb morphogenesis. *Hand2* is expressed in the posterior portion of the developing limb buds in the signaling region called the zone of polarizing activity (ZPA) (Charite et al., 2000, Fernandez-Teran et al., 2000). It has been implicated that retinoic acid signaling first establishes *Hand2* in the ZPA (Mic et al., 2004). *Hand2* can upregulate expression of *Sonic Hedge Hog* (*Shh*) in the ZPA and expression of *Shh* upregulates expression of *Hand2*. Overexpression of *Hand2* in the limb buds results in polydactyly associated with expanded *Shh* expression which results in ectopic ZPA formation (Charite et al., 2000, Fernandez-Teran et al., 2000, McFadden et al., 2002) while *Hand2*-null embryos lack any detectable *Shh* expression domain (Charite et al., 2000). *Hand2* also upregulates the BMP antagonist *Gremlin,* which acts to maintain an *Shh*/FGF feedback loop that maintains the ZPA (McFadden et al., 2002, Zuniga and Zeller, 1999). The *Shh* repressor *Gli3* helps to restrict *Hand2* expression to the ZPA, which in turn feedbacks to regulate *Gli3*, allowing *Shh* signaling (Liu et al., 2005). Additional factors that potentially regulate *Hand2* in the limb are *Tbx3*

and *Hoxd13* and due to their coexpression Twist1 (Rallis et al., 2005, Salsi et al., 2008 Firulli et. al., 2005).

Hand2 is expressed in multiple derivatives of neural crest cells, including the peripheral nervous system. Specifically, *Hand2* has been implicated in specification and maintenance of the noradrenergic phenotype of the sympathetic nervous system and chromaffin cells of the sympathoadrenal lineage development (Huber et al., 2002, Xu et al., 2003). Ectopic expression of *Hand2* is capable of activating the noradrenergic program (Howard et al., 1999, Morikawa et al., 2005). BMP's have been implicated in activating the noradrenergic phenotype and several of the transcription factors regulating sympathetic differentiation, including *Hand2* (Howard et al., 2000, Liu et al., 2005b, Muller and Rohrer, 2002). Unlike other transcription factors expressed during sympathetic neurogenesis that are responsive to BMP's which include *Phox2a, Phox2b,* and *Mash1,* only *Hand2* is exclusive to noradrenergic differentiation. Cilliary neurons lacking *Hand2* expression become cholinergic in response to BMP (Muller and Rohrer, 2002). Additionally, mesenchephalic neural crest cells that are *Hand2*-negative cannot differentiate into catecholaminergic neurons (Lee et al., 2005).

These studies suggest a role for *Hand2* specifying and maintaining the noradrenergic phenotype during catecholaminergic differentiation. Additional evidence to support this hypothesis is that *Hand2* directly transactivates *Dopamine β-Hydroxylase* (*DBH*) in conjunction with *Phox2a* (Rychlik et al., 2003,

Xu et al., 2003). Conditional knockouts of *Hand2* in neural crest cells reveals that sympathetic precursors differentiate into neurons but fail to express noradrenergic biosynthesis enzymes, such as *DBH*, further suggesting a role in the determination of the catecholaminergic phenotype (Hendershot et al., 2008, Morikawa et al., 2007). In the enteric nervous system, gain-of-function of *Hand2* *r*esults in an overall increase of neurogenesis, suggesting it may have the potential to drive the noradrenergic phenotype; however, *Hand2* loss of function suggests that *Hand2* neural crest migrate properly and express neurogenic markers but fail to terminally differentiate, again suggesting a role for *Hand2* in specification and maintenance of the noradrenergic phenotype (D'Autreaux et al., 2007, Hendershot et al., 2007). In Zebrafish, there is only a single hand gene most identical to *Hand2.* A mutation of *Hand2*, called *Hands off*, shows that sympathetic precursors migrate properly and undergo proper neurogenesis, but ultimately fail to express noradrenergic genes indicative of terminal differentiation of catecholaminergic neurons (Lucas et al., 2006).

As with all *Twist*-family bHLH's, *Hand2* is capable of forming heterodimers with E proteins to regulate transcription (Dai and Cserjesi, 2002). Though E-proteins are near ubiquitously expressed in embryonic tissue, they are expressed at lower levels in the heart, suggesting that Hand2 potentially dimerizes with other bHLH proteins or other factors to regulate development in heart tissue (Murakami et al., 2004). Among these potential dimer partners, it has been shown that Hand2 can heterodimerize with Hand1 and potentially acts as an

inhibitor, imparting a multifunctional role on Hand factors (Firulli et al., 2000). GATA4 has also been shown to synergize with Hand2 to activate *Anf* through a direct interaction with P300 (Dai et al., 2002). The ability of Hand2 to transactivate is enhanced through stabilization when bound to DNA by JAB1 (Dai et al., 2004).

Phosphoregulation also regulates dimerization of Hand2. As previously discussed in *Twist1*, phosphorylation alters the dimerization preference of *Hand2*, mediated by PKA, and directly influences the antagonistic relationship with *Twist1* (Firulli et al., 2003, Firulli et al., 2005). BMP's regulate Hand2 via induction of PKA, which phosphorylates the conserved helix 1 threonine and serine promoting noradrenergic differentiation from a specified cell type (Liu et al., 2005).

Cre Recombinase as a Necessary Tool for Lineage Conditional Studies

Conventional gene targeting generates a mutant allele in all cells of the mouse following fertilization. This serves as an extremely useful tool for investigating gene function during development. However, difficulties can be encountered, such as embryonic lethality, and analysis can be complicated due to indirect effects from ablating the gene in all tissues. The P1 bacteriophage protein Cre is capable of mediating site specific recombination at *loxP* sites found in their genome and has applications for use in the mammalian system. To date, the Cre-*loxP* system is the best characterized means of achieving conditional

gene inactivation in mice and has contributed extensively as a tool for altering the mammalian genome.

Site-specific recombination mediated by the integrase family of enzymes plays a central role in the life cycles of temperate bacteriophage, bacteria, and yeasts (Landy, 1993). This includes the integration into and excision from the host chromosome of phage genomes, in stable partitioning of plasmid, phage, or bacterial genomes, in effecting developmental switches in gene expression and in the copy number control of yeast plasmids via replication amplification (Yoziyanov et al., 1999). The P1 bacteriophage site-specific recombination event mediated by *Cre* and its recognition sites (called *loxP*) were originally identified through a series of mutagenesis studies in the early 1980's (Sternberg and Hamilton, 1981). For most of the decade, the mechanism surrounding Cre-mediated recombination and its interaction with the *loxP* site were vigorously studied and ultimately delineated. Though Integrase type recombinase have not been found in higher Eukaryotes, the research of Professor Brian Sauer while at DuPont lead to the development of the Cre-*LoxP* recombinase technology and its functional application in the eukaryotic genome after a series of *in vitro* cell culture experiments in PK15 cells (Sauer and Henderson, 1988). These experiments were followed by the demonstration that the Cre recombinase worked *in vivo* when a transgenic Cre mouse line was used to activate a dormant transgene flanked by *loxP* sites, causing tumorigenesis (Lasko et al., 1992). Ultimately the development of the Cre-*loxP* recombinase system has

revolutionized mouse genetics by proving to be an essential tool for conditional genetic alteration in mice.

The Cre Recombinase Protein Catalyzes Site-Specific Recombination of loxP sites

Integrase family members cleave their DNA substrates by a series of staggered cuts (Guo et al., 1997). Very little sequence similarity is shared between these members, except for four residues required to catalyze the reaction (Abremski and Hoess, 1992). It has been suggested that the dissimilarity of sequence between Integrase family members is due to the overwhelming diversity in the function and manner in which these proteins carry out their recombination function. The lysogenic phase is characterized by the fusion of the nucleic acid of a bacteriophage with that of a host bacterium. The newly integrated genetic material, called a prophage, can be transmitted to daughter cells at each subsequent cell division (Ikeda and Tomizawa, 1968).The role of the Cre recombinase in the P1 bacteriophage has been to maintain the phage genome as a monomeric, single-copy plasmid in the lysogenic state and aid in the circularization of the linear P1 DNA following infection and the breakdown of P1 dimers that form during recombination following replication (Abremski et al., 1983).

The Cre-*loxP* site-specific recombination system of bacteriophage P1 consists of a site at which recombination takes place, *loxP*, and a phage encoded

protein that mediates the reaction, Cre (Sternberg and Hamilton, 1981). The Cre recombinase of the P1 bacteriophage belongs to the integrase family of site-specific recombinases. Integrases are enzymes that facilitate the sequential exchange of DNA strands resulting in an chromosomal integration or excision event. Some examples include: λ Integrase, HP1 Integrase, XerD and Flp in addition to Cre recombinase. Cre is a 38kD protein, encompassing 341 amino acids (Hamilton and Abremski, 1984). It is comprised of 4 subunits with a N-terminal and C-terminal domain. The C terminal domain serves as the catalytic site of the enzyme (Guo et al., 1997).

LoxP is a site on P1 bacteriophage DNA where recombination occurs and is the substrate for the Cre recombinase protein which catalyzes recombination between two sites. The *loxP* site is 34 base pairs in length and consists of two 13 base pair inverted repeats separated by an 8 base pair spacer region (Hoess et al., 1986). The perfect 13 base pair repeats impart the directionality of the *loxP* site on the spacer region. Another DNA integration site is found in P1 called *loxB*. Though Cre can mediate integration at this site, it occurs at a very low frequency compared to the extraordinary efficiency of the *loxP* site as determined in paired phage crosses (Abremski et al., 1983; Sternberg and Hamilton, 1981).

Cre recombinase binds to the *loxP* site to initiate recombination. When DNA containing the *loxP* site is incubated with the Cre enzyme, specific cleavage occurs within the spacer region, creating a six base-pair staggered cut during

recombination (Hoess and Abremski, 1985). The cuts are centered on the axis of symmetry between the two strands and results in a protruding 5' end:

$^{5'}$ A↓T-G-T-A-T-G C $^{3'}$

$^{3'}$ T A-C-A-T-A-C↑G $^{5'}$

The placement of the cut two base pairs from the end of the spacer sequence coincides with the region of strand exchange. The relationship of the cleavage site to the location of the strand exchange strongly argues against the cleavage products being randomly generated by Cre.

During recombination two Cre recombinase molecules becomes covalently attached to the 3' end of each DNA strand at the point of cleavage. Each Cre protein contacts the 15 outermost base pairs and the first 2 base pairs of the spacer region (Guo et al., 1997). Deletion experiments have shown that sequences outside of the inverted repeats of *loxP* can be removed without loss of recombination. Furthermore, base pair mutations within either homologous arm or within the 2 base pairs of the spacer confirm that they are required for recombination to occur suggesting that these sites are necessary for Cre interaction at *loxP* (Hoess et al., 1986).

Though the Integrase family of recombinases shares little amino acid homology, secondary structural alignments indicate a large conservation of peptide motifs within which specific residues have been retained throughout the family. Specifically, they contain a four amino acid conserved region consisting of two arginines, one histidine, and one tyrosine (Guo et al., 1997). The tyrosine residue is responsible for breaking the DNA chain to form a 3'-phosphotyrosine bridge and expose an adjacent 5' hydroxyl. This frees up the 5'-OH of cleaved strand. The phospho-tyrosine bond then becomes the target of attack by the 5'-hydroxyl group from the cleaved strand of the partner DNA during the strand joining step of recombination group (Yoziyanov et al., 1999).

Cleavage resulting in a break of a phosphodiester bond 3' to the phosphate and simultaneous covalent attachment between DNA and protein is a feature shared with other topoisomerases and is a means by which bond energy is preserved following cleavage to allow for rejoining without an external energy source (Hoess and Abremski, 1985). Since Cre recombinase is the only protein required and the reaction does not require an external energy source, it is a very efficient reaction. Early experiments using an EcoRI restriction fragment containing flanking *loxP* sites showed that Cre recombinase could efficiently and specifically excise the flanked DNA fragment (Sternberg and Hamilton, 1981). The independence from energy co-factors and the high fidelity of the reaction make this an extraordinarily sound system to initiate recombination.

Cre recombinase is capable of mediating recombination at *loxP* sites. The specific action that takes place ultimately depends on the orientation of two *loxP* sites with one another. Deletion experiments have shown that the region flanking the *loxP* sites are not important for the recombination event to occur (Hoess et al., 1986). Since the *loxP* site contains two palindromic arms, directionality is ultimately determined by the spacer sequence. The cleavage event creates a 6 base pair overhang that requires a specific configuration to bind the reciprical strand. In the event that the *loxP* sites are located in the same orientation and on the same strand, the flanked DNA will be excised in a circular fashion. The Cre molecules bound to the C-terminal *loxP* site will loop to form an intermediate interface with the N-terminal *loxP* sites that is stabilized by the Cre-DNA interactions before the recombinases join the flanking strands and excise the flanked DNA (Guo et al., 1997). In the event that the *loxP* sites are positioned in an opposing orientation, the cleaved strands will only be able to join in such a manner as that it causes an inversion of the flanked DNA.

Cre-loxP Recombinase Is A Powerful Reagent For Tailoring The Genome

The highly specific relationship and function coupled with the efficiency of the reaction makes the Cre-*loxP* recombinase a powerful application in the mouse genome. The mammalian genome does not contain Integrase type site specific recombinases (Nagy, 2000). Therefore, the application of the Cre recombinase system is reliant on the absence of *loxP* sites in mice. The random occurrence of a specific 34 base pair sequence requires a 10^{18} base pair length

of DNA. The entire mammalian genome is only 3 X 10^9 base pairs (Nagy, 2000). This suggests that it is highly unlikely that a *loxP* site will be present outside of the phage genome. Therefore, the introduction of *loxP* sites to the eukaryotic genome will be highly specific and in combination with Cre should allow the achievement of specific genome alterations.

Cre recombinase is only one member of an entire family of integrase recombinases. There are other family members that are also independent of energy co-factors and that exhibit a high frequency of recombination, such as Flp recombinase. Flp recombinase has been used successfully in *Drosophila*. However, these recombinases have a disadvantage in that they are not as effective in the mammalian genome (Rossant and McMahon, 1999). One problem may be that the Flp protein is not be optimized for use in the mammalian cell. Flp recombinase does work and serves a role in mammalian cells on the ES cell level in the removal of a selectable marker. Further developments in the enhancement of Flp recombinase hold promise for optimal use in the mammalian genome.

One use for the Cre-*loxP* recombinase system is the removal of selectable markers. Classical gene targeting relies upon the use of a positive selection marker in the targeted locus for ES cell selection to generate a systemic knock-out. It must always be considered that selection marker expression from this locus could potentially affect the mutant phenotype. Flanking the positive selection marker, such as neomycin, with *loxP* sites allows for the excision of the

selection marker following the identification of the properly targeted allele. Transient expression of Cre recombinase *in vitro* works efficiently to remove the selection marker and provides the advantage of a clean allele with which to study (Sauer and Henderson, 1988).

The most anticipated and obvious use for the Cre-*loxP* recombinase system comes from the ability to generate conditional or cell-type specific mutagenesis of the muse genome. There are several reasons for this. First and foremost, systemic germline mutations have the overwhelming potential to be lethal. In this event, there is no mouse to study. Secondly, a gene may be expressed in different developmental programs and in different cell types. In this case, the systemic knock-out presents a complex phenotype that may be riddled with secondary defects that are compounding a phenotype. Essentially, this creates a situation where the initial stages in which the gene plays a role but not necessarily the later stages may be available for concrete analysis.

The strategy for the conditional targeting of genes is to flank a target gene or gene segment with *loxP* sites in ES cells by classic gene targeting and deleting the selection marker gene by transient transfection with a Cre or Flp expressing plasmid (Nagy, 2000). This results in a mutant mouse carrying a functional, *loxP* flanked gene. To remove the selection marker, either three-loxP sites can be used or flanking the selection marker with *frt* sites for excision using a Flp expressing plasmid is an alternative. Though this is a simple idea, there are serious potential problems, which can be encountered. The most relevant

problem is that the *loxP* sites need to be targeted in such a manner that they can delete critical regions of DNA such that protein function is ablated. The safest manner in which to do this is to flank the entire gene, though this can be meet with great difficulty in large (<100kb) multi-exon genes. In light of this event, flanking of a vital exon, one encoding the translational start, is a proven alternative approach. The second problem that requires serious consideration is that the unrecombined gene be kept fully functional. Problems can be encountered when the *loxP* site is targeted into the middle of a conserved regulatory element, which can affect normal gene regulation.

The conditional knockout of a gene can be achieved by crossing the conditional mutant animal with a Cre transgenic mouse line or one expressing Cre recombinase targeted to a genes endogenous regulatory elements. The advantage of placing Cre under control of a lineage specific promoter is that it achieves a spatial restriction of recombination, allowing researchers to more accurately address their questions by pinpointing specific cell types. This system can achieve further enhancement when a Cre recombinase is fused to a mutated estrogen receptor, which has lost its ability to bind estrogen but can still bind the antagonist tamoxifen (Danielian et al., 1998). The nuclear localization capabilities of estrogen allow the researcher to regulate Cre expression in a temporal manner and address the multiple roles of gene function at different time points in development or to circumvent embryonic lethality.

There are certain limitations and considerations when using a Cre expressing mouse line. The first is whether the Cre line is sufficient to recapitulate endogenous gene expression and to drive Cre at a high enough level for excision to take place. Transgenic mice can often encounter difficulties with poor expression as a result of their random integration while Cre needs to be expressed at a sufficiently high enough level for recombination to occur. Therefore there may be a degree of mosaiscim in expression where excision may not be 100% efficient. Additionally, one must consider the extent to which the promoter element overlaps the endogenous gene expression and whether the gene of choice will be expressed in all cells. For instance, there are multiple neural crest Cre drivers, however, each of them has a unique expression profile that when used to delete a specific genes can result in a range of phenotypes. An additional consideration is that the Cre-mediated excision event takes time and is not an instantaneous event. The Cre protein has to be translated and built up to a sufficient level to ensure that an excision event takes place. Following excision the gene of interest will be eliminated, but some mRNA may still linger for translation. This means that there should be a delay between the onset of Cre transcription and the actual biological effects which researchers need to consider (Nagy, 2000).

The Cre-*loxP* system has been utilized for the generation of conditional activation expression mice. Initially this approach was used to generate reporter mice that would permanently mark real-time expression as well as all daughter

cells derived from these expressing cells. These mice contain a *loxP*-STOP cassette that interrupts transcription of a reporter gene such as β-galactosidase or eGFP/eYFP/eCFP. Targeting of this construct to a ubiquitously expressed allele has enabled the research community to fate map specific cell lineages with the appropriate Cre-driven mouse line. Upon excision, the ubiquitous promoter elements direct control of the reporter gene. Since this is an alteration of the genomic DNA, this alteration is permanent, allowing the reporter to be expressed permanently following the transient activity of Cre recombinase. The ubiquitous Rosa-26 gene trap integration site has been successfully targeted with a series of Cre excision conditional reporters that have been shown to work successfully as a reporter (Soriano, 1999). Furthermore, conditionally active alleles can be generated using the STOP cassette strategy.

The Cre-*loxP* system has shown that it is a valuable tool for genetically altering mice. It has enabled the research community to achieve optimization of spatial and temporal expression of genes as well as the ability to fate map cell lineages in mice – something once exclusive to avian and zebrafish. The mechanism that Cre operates by allows it to perform efficiently on the mammalian genome without imparting its own phenotypic effect. In light of the benefits within Cre recombinase, the potential problems and downfalls that are encountered with the Cre-*loxP* system must always be considered. Generation of Cre and conditional *loxP* mice are often more laborious that in traditional cloning. The multitude of parts and different alleles presents many opportunities

for careless oversight to create technical difficulties. However, properly designed experiments should not face these difficulties and should leave the researcher with a set of powerful genetic tools to conduct experiments.

Hand1 Lineage Analysis

Generation of *Hand1*$^{EGFPCre\Delta Neo/+}$ mice

To follow the fate of cells that express *Hand1,* we targeted an *eGFPCre* fusion protein expression cassette to the *Hand1* locus in a murine ES cell line via homologous recombination (Fig. 1A). Following neomycin selection, targeting was confirmed in ES cell clones via Southern blot analysis (Fig. 1B). Properly targeted ES cells display a single 10Kb *Cre* cassette-containing *EcoRI* RFLP in the absence of secondary sites of insertion (Fig. 1C). Two targeted ES clones were injected to host blastocysts to generate first chimeric mice and then germline *Hand1*$^{EGFPCre\Delta Neo/+}$ allelic transmission. Removal of the *neomycin* resistance cassette, via intercross with *FLPeR* mice (Farley et al., 2000), resulted in a detectable *Hand1*$^{EGFPCre\Delta Neo/+}$ RFLP size shift (Fig. 1D). Both mouse lines expressed *Cre* identically, and we thus employed only one of these lines for these studies. *eGFP* mRNA expression, detected via *in situ* hybridization, correlates precisely with that of *Hand1* (Fig. 1E,F). *Hand1*$^{EGFPCre\Delta Neo/+}$ mice are viable and fertile but must be maintained as heterozygotes as homozygotes are null for *Hand1* and thus die embryonically (Firulli et al., 1998).

The *Hand1* Lineage contributes to a subset of the FHF and epicardium

To test the fidelity of the *Cre* expression in *Hand1*$^{EGFPCre\Delta Neo/+}$ mice, we intercrossed *Hand1*$^{EGFPCre\Delta Neo/+}$ males with *R26R-β-galactosidase (*β-gal) homozygous female mice and compared β-gal reporter activity with both real

time *Hand1* mRNA expression and β-gal activity from the *Hand1*^{LacZ} allele (Fig. 2). At E9.5, both whole-mount and section analyses shows no significant difference between real-time and *Hand1*-lineage expression (Fig. 2A,E,I,C,G, and K). As expected, both *Hand1* expression and lineage mark the First heart field (FHF) derived left ventricle, showing little expressional overlap with the *Hand2*-expressing SHF (Morikawa and Cserjesi, 2008). Interestingly, at E10.5 *Hand1*-lineage departs from real-time *Hand1* expression. In whole mount, the entire heart appears to be *Hand1*-lineage positive, which would superficially suggest an upregulation of *Hand1* within the SHF (Fig. 2F). However, section analysis discounts this observation, revealing a right ventricular myocardium largely devoid of LacZ activity (Fig. 2K). Rather, the epicardium is robustly LacZ stained in *Hand1*$^{EGFPCre\Delta Neo/+}$ embryos in contrast to *Hand1*$^{LacZ/+}$ embryos, which show no detectable epicardial LacZ staining (Fig. 2H). Thus, cells that expressed *Hand1* during their maturation ultimately contribute to cardiac epicardium.

We then examined E15.5 and adult myocardial tissues to assess the contributions of the *Hand1*-lineage to both the late embryonic and the fully formed heart (Fig. 3A-B). At these stages, the *Hand1*-lineage continues to mark a portion of the inner wall of the interventricular septum (IVS) and the left ventricular myocardium. LacZ staining is not detected in adult atrial cardiomyocytes, indicating that the *Hand*-lineage does not mark cardiomyocytes within the entire FHF, but only a subset that contributes to the left ventricle. Consistent with earlier time points, SHF derived right ventricular myocardium shows no evidence of *Hand1*-expression and, with the exception of a small

population of SHF derived cardiomyocytes within the myocardial cuff, there is a near exclusion of *Hand1* expression from this population of pharyngeal mesoderm-derived *Hand2*-expressing myocardium (McFadden et al., 2000; Srivastava et al., 1995).

Both *in situ* hybridization and *Hand1*^{LacZ} staining fail to detect *Hand1* within the endocardial or epicardial lineages. We performed immunohistochemistry to detect co-expression of Flk1, a marker of both of these cell types, and *Hand1*$^{EGFPCre\Delta Neo/+}$ activated eGFP fusion protein to carefully examine whether the *Hand1*-lineage contributes to the endocardium or coronary endothelium (Fig. 3C-H). Consistent with the lack of detectable real-time expression, no Flk1-positive endocardial or coronary vessel cells coexpressed eGFP.

LacZ staining of the *Hand1*-lineage was also not detected within the atrial myocardium. Immunohistochemistry for the *Hand1*-lineage did not mark the atrial myocardium, validating this observation (Fig. 3I-K). Together, these data provide a new perspective on the contributions of *Hand1*-expressing lineages to the heart where, with the exception of the myocardial cuff, *Hand1* is excluded from SHF myocardium, is restricted to a ventricular subpopulation of the FHF, and marks both the progenitors and derivatives of the proepicardial organ and epicardium. More importantly, these data define more restricted spatiotemporal expression overlap with the related Hand1-interacting factor, *Hand2*.

The *Hand1*-lineage marks specific subpopulations of cranial, cardiac and trunk neural crest, but not vagal/sacral neural crest

Hand1 and *Hand2* expression is observed within subpopulations of cranial, cardiac, trunk, and vagal/sacral NCCs that contribute to the jaw, cardiac OFT, sympathetic nervous system and enteric nervous system, respectively (Abe et al., 2002; Barbosa et al., 2007; Hendershot et al., 2008; Holler et al., 2010; Morikawa and Cserjesi, 2008; Morikawa et al., 2007; Yanagisawa et al., 2003). This expression can be observed in whole mount *Hand1*^{LacZ} expression at E12.5 (Fig. 4A). Craniofacial expression of *Hand1* at E12.5 is restricted to the midline of both the developing tongue and the mandibular process, and at E14.5 it is still expressed in the midlines of both the tongue and the Meckel's cartilage in the mandible (Fig. 4B, C, E, and F). Comparisons of real-time *Hand1* expression to the *Hand1* craniofacial lineage at E14.5 show that the *Hand1*-lineage marks a wider subset of tissue within the tongue and the entirety of Meckel's cartilage in the mandible (Fig. 4D, G). This suggests that *Hand1* may influence formation of midline features of both the tongue and lower jaw.

Hand1 real-time expression within the OFT and pharyngeal arches of E10.5 mouse embryos is subtly distinct from that of the *Hand1*-expressing cNCC lineage (Fig. 4H, I). Medial cNCC within the forming aortico-pulmonary septum show an indistinguishable distribution of *Hand1*-expressing/marked cells. However, *Hand1*^{LacZ} expression is observed in approximately 50% of cNCC occupying the OFT, while almost all of these cells are marked as having derived from the *Hand1*-lineage suggesting that *Hand1* real-time expression is

downregulated as cNCC migrate into the OFT (Fig. 4B). This finding is consistent with previously published observations (Vincentz et al., 2008).

Hand1 expression marks trunk NCC-derived neurons within the sympathetic ganglia (Cserjesi et al., 1995; Firulli et al., 1998; Hollenberg et al., 1995). Comparison of *Hand1* expression with that of the *Hand1*-lineage shows little variation (Fig. 4J, K). *Hand1*$^{Lacz/+}$ E18.5 embryos show robust β-gal staining within the sympathetic chain (Fig. 4J), and this expression persists in adults (data not shown). *Hand1*-lineage is consistent with this expression (Fig. 4K).

Finally, we looked at the *Hand1*-lineage within the vagal/sacral NCC-derived cells of the enteric nervous system and gut at E12.5 and 14.5 (Fig. 4L-N, P-R). *Hand1* expression was found in the smooth muscle component of the midgut and hindgut. At E14.5, the *Hand1*-lineage robustly marks both the submucosa of the duodenum, a smooth muscle cell subpopulation surrounding the muscilaris externa, and the outer connective adventitia. The *Hand1*-lineage is absent from villus epithelium. Additionally, the *Hand1*-lineage is detected within the posterior vein and the bile duct, as well as the surrounding connective tissue. Comparison of the *Hand1*-lineage to the *Wnt1*-lineage at E14.5 indicates that the *Hand1* lineage is excluded from the NCC components of the enteric nervous system but does mark lateral mesoderm structures of the gut (Fig. 4Q, S).

The *Hand1*-lineage shows varying contributions to the developing fore- and hindlimbs

Hand1 is expressed, beginning at E11.5, within the anterior-ventral domain of the developing mouse limb and, by E13.5, is restricted to digit 1 (Fernandez-Teran et al., 2003). *Hand1* is also expressed within the lateral mesoderm medial to the forming limb buds. Compared to *Hand2*, limb expression *Hand1* is greatly restricted; however, expression of these two related factors does partially overlap (Fernandez-Teran et al., 2003; Firulli et al., 2005).

Forelimb expression of *Hand1* at E9.5 and E10.5 appears in the lateral mesoderm underlying the forelimb bud (Fig. 5A,E). Lineage analysis marks this lateral mesoderm in addition to clonal cell populations within the limb bud (Fig. 5B). At E10.5 the *Hand1*-lineage marks a subset of cells that contribute predominantly to the ventral side of the limb bud, indicating that *Hand1*-positive cells in the lateral mesoderm contribute to limb bud development in a pattern-specific manner (Fig. 5F).

Meanwhile, hindlimb expression of *Hand1* at E9.5 marks the both the lateral mesoderm and the ventral mesenchyme of the limb bud (Fig. 5C). The *Hand1*-lineage at E9.5 marks, in addition to the ventral and lateral mesoderm derived cells, a considerable subset of mesenchymal cells occupying the dorsal compartment of the limb bud (Fig. 5D). At E10.5, *Hand1* hindlimb expression becomes restricted to the lateral mesoderm, while we see a broad expansion of the *Hand1*-lineage throughout the hindlimb mesenchyme. This indicates that both

dorsal and ventral hindlimb mesenchyme receive an early and substantial contribution of *Hand1*-expressing cells.

Hand1 expression is considerably downregulated within the limb bud by E10.5. Whole mount analysis of *Hand1*^{LacZ} at later stages confirms, as has been previously reported, a late domain of expression at E12.5 in both the fore- and hindlimbs (Fig. 5I,K) (Fernandez-Teran et al., 2003). This expression of *Hand1* is downregulated in the limb by E14.5 (Fig. 5M, N). Lineage analyses at E12.5 and E14.5 confirm contribution of *Hand1*-expressing cells to the limbs with, as expected, comparatively more extensive staining in the hindlimb, (Fig. 5J, L, N, P). Importantly, these experiments indicate that there are two separate expression domains of *Hand1* within the developing limb. First, there is an early expression domain, detectable during stylopod formation, largely within the lateral mesoderm and the ventral forelimb bud. Surprisingly, derivatives of these early *Hand1*-expressing cells contribute extensively to the limb bud mesenchyme. Second, there is a late expression domain of *Hand1* that is crucial for digit formation during autopod maturation (Fernandez-Teran et al., 2003). Together, this data indicates that the expression and contribution of *Hand1* during limb formation is more dynamic than previously thought.

The *Hand1*-lineage contributes to the extra embryonic mesoderm and trophoblasts during placental development

Hand1 null mice die between 8.5 and 9.5 due to defects in extra embryonic and vascular tissues (Firulli et al., 1998; Morikawa and Cserjesi, 2004;

Riley et al., 1998). Contributions of the *Hand1*-lineage to the placenta and associated vasculature were assessed at E9.5, and E14.5 (Fig. 6). As expected, at E9.5 the *Hand1*-lineage marks the chorion, allantois, yolk sac, and trophoblast giant cells (Fig. 6A-D), and is not observed within the decidua (Fig. 6A, C). At E14.5, after the specific layers of the placenta have formed, the *Hand1*-lineage contributes, in addition to yolk sac and chorion, to the amnion, both the endothelium and the smooth muscle of the umbilical vein, Wharton's jelly, which surrounds and insulates the developing umbilical chord, the vitiline vessels, a heterogeneous cell population within the placental labyrinth and the trophoblasts with the anterior domain of the spongy layer (Fig. 6E-H). To identify these *Hand1*-lineage-postive cells within the labyrinth, immunohistochemistry was performed using eGFP, Flk1 and αSMA antibodies at E12.5 (Fig. 6I-P). A complete overlap of eGFP and Flk1 immunoreactivity is observed, suggesting that the *Hand1*-lineage marks the vascular endothelium, where as the complimentary pattern of αSMA suggests that smooth muscle within this domain derives from cells independent of *Hand1*-expression. Real-time *Hand1* expression is indistinguishable from *Cre* expression at these stages (data not shown). Taken together, these data show that cells which do express or which have expressed *Hand1* compose nearly all trophoblasts and components of the extraemrbyonic vasculature as well as a significant portion of the labyrinth endothelium.

Hand1 marks vascular structures derived from lateral mesoderm

At E9.5 and 10.5, real-time *Hand1*^{LacZ} staining clearly shows lateral mesoderm-restricted expression (Fig. 7A-B). In contrast, *Hand1*-lineage analysis at these time points reveals cells migrating out of the lateral mesoderm between the somites (Fig. 7C-D). Close examination suggests that these cells are forming the vascular plexus of the intersomitic vessels. CD31 (PECAM) antibody staining confirms that these *Hand1*-lineage cells are vascular endothelium (Fig. 7C-F). Comparison between the *Hand1*, lineage and the *Wnt1-Cre* lineage confirms the *Hand1* lineage marked vascular endothelium is derived from the lateral mesoderm and not the NCC lineage (Fig. 7G-H). No *Hand1*-linage contribution was observed rostral to the forelimb, indicating that the vascular progenitors of these vessels are independent of *Hand1* expression (data not shown).

To more precisely characterize *Hand1* vascular contributions, we examined the *Hand1*-lineage within caudal sections of E9.5 day embryos (Fig. 8). *Hand1*-linage cells are readily detectable in the caudal endothelium of the dorsal aorta (Fig. 8B, D). Interestingly, at E14.5 the Flk1-positive endothelium of the distal dorsal aorta (Fig. 8G, K) is composed of a mix of both *Hand1*-lineage, detected by expression of eGFP (Fig. 8G, K), and non-lineage cells (Fig. 8H, L). *Hand1*-lineage cells are not observed within the endothelium of the proximal dorsal aorta (data not shown) but can be observed in small populations within the vessels that increase in number moving caudally from the forelimb. Interestingly, the *Hand1*-lineage also marks a small population of blood cells (Fig. 8D, L). It is likely that the extensive *Hand1*-expressing cells within extra embryonic structures

and the lateral mesoderm respectively contribute to blood islands within the yolk sac and, potentially, blood cells that populate the liver. Given that the *Hand1*-lineage contributes to endothelium of both the intersomitic vessels and the dorsal aorta, we conclude that components of the caudal vasculature and some hematopoietic cells derive from *Hand1*-expressing progenitors.

Chapter Two

Hand2 Deletion in the *Hand1* Lineage

Dynamic Expression of Hand factors during Heart Morphogenesis

E8.5 linage analysis of *Hand1* reveals that the linear heart tube is not completely derived from *Hand1*-expressing cells. To account for a temporal delay of *Cre* expression, we performed whole mount ISH for *Hand1* at E7.5. *Hand1* is detected throughout the extra embryonic mesoderm, chorion, and allantoic rudiment (Fig. 9A). As the chorion is directly adjacent to the cardiac crescent (Fig. 9A,B white arrow), we performed a double label *ISH* for both *Hand1* and the cardiac marker *Mlc2a* (Cai et al., 2003). Results show that *Hand1* does not overlap with *Mlc2a* heart expression at E7.5, suggesting that *Hand1* expression initiates in cardiomyocytes subsequent to linear heat tube fusion (Fig. 9B).

To further delineate early Hand factor expression during cardiogenesis, we performed *ISH* for both *Hand1* and *Hand2* at E8.5 (Fig. 9C-F). Whole mount *ISH* shows expression of *Hand1* in the posterior heart tube while *Hand2* is expressed throughout the entire cardiac field. Sagital sections show *Hand1* expression restricted to myocardium of the early ventricular chamber and absent from the OFT. *Hand2* expression is throughout the endocardium and mesoderm of the SHF and OFT. However, *Hand2* is not detected in the myocardium of the ventricular chamber at E8.5 (Fig. 9F, red arrow). There is observable overlapping

expression within the SHF-derived OFT myocardium of the cuff and spatiotemporal overlap within the left ventricle FHF myocardium, suggesting that Hand factors may be functionally overlapping within these domains during cardiogenesis. Together, this indicates that Hand factors are dynamically regulated and lack significant overlapping expression profiles during early heart morphogenesis showing coexpression only within the SHF-derived myocardium of the cuff.

Hand2 ablation within the *Hand1*-lineage results in novel phenotypes and embryonic lethality

Hand1-lineage analysis and Hand factor *ISH* reveals that Hand factors display largely complementary heart expression profiles, suggesting that both *Hand1* and *Hand2* exhibit unique functions during cardiogenesis. To explore potential functional overlap, we ablate *Hand2* within the *Hand1* lineage (*H2CKO*) via intercross of $Hand2^{fx}$ (Morikawa and Cserjesi, 2008) and $Hand1^{Cre}$ mice. *Hand1* and *Hand2 ISH* of *H2CKO* OFTs at E10.5 show successful ablation of *Hand2* within the *Hand1* domains of pharyngeal arch mesenchyme, lateral mesoderm contributing to the OFT myocardium, NCC-derived mesenchyme populating the OFT, and posterior lateral mesoderm (Fig. 9G-L).

H2CKO embryos were recovered at slightly below expected Mendellian ratios thru E12.5 (Fig. 10). At E14.5, *H2CKO* embryos were recovered; however, roughly 50% of the *H2CKOs* collected were dead. No viable *H2CKOs* were collected past E14.5. *H2CKOs* displayed slight patterning defects along the A-P

axis of the limbs at E12.5 (data not shown), but otherwise appeared phenotypically normal. Patterning of the heart, function of *Hand1*, and cardiomyocyte differentiation is normal (data not shown). However, a multitude of defects are observed by E14.5 in *H2CKOs*.

H2CKOs display pericardial hemorrhaging, anasarca, liver hypoplasia, syndactyly of the hindlimbs, and oligodactyly of the forelimbs (Fig. 10A-D, G-H). OFT septation defects, including Persistent Truncus Arteriosus (PTA) and Double Outlet Right Ventricle (DORV), are observed in all *H2CKOs* and suggest defects within cNCCs and/or SHF-derived myocardium (Fig. 10E-F,I-L). Hypertrabeculation/noncompaction and VSDs indicate *H2CKOs* suffer from severe cardiovascular defects that in isolation should result in neonatal lethality (Fig. 10M-P).

Hand2$^{\Delta NCC}$ die from a failure of the peripheral nervous system to synthesize norepinepherine prior to E12.5(Morikawa and Cserjesi, 2008). Given that *Hand1* is expressed within a subset of NCCs, it is possible that *H2CKOs* also die due to defects within the sympathetic nervous system. *Hand2*$^{\Delta NCC}$ embryos can be rescued postnatally with the administration of the β-adrenergic agonist isoproterenol (Morikawa and Cserjesi, 2008). *H2CKOs* administered isoproterenol, in contrast to *Hand2*$^{\Delta NCC}$ embryos, failed to survive till birth (Fig. 11), indicating that sympathetic nervous system-related defects do not significantly contribute to *H2CKO* embryonic lethality.

Hand1 expression within the septum transversum marks the progenitors of the proepicardium

As *Hand1*-lineage cells are observed in the epicardium at E10.5, we examined *Hand1* expression within the PE. The PE is derived from the anterior surface of the septum transversum (ST) and gives rise to the epicardium (Watt et al., 2004). *ISH* were conducted for both *Hand1* and *Tbx18*, a marker of the PE, at E9.5 (Cai et al., 2008; Christoffels et al., 2009) (Fig. 11A-E). *Tbx18* is expressed throughout the PE but is not within the ST. *Hand1* expression is not detectable within the PE but is expressed robustly throughout the ST. X-Gal staining of the $Hand1^{LacZ}$ confirms expression distinctly in the LV and the ST (Fig. 11F). X-Gal staining of the *Hand1* lineage shows that *Hand1*-marked cells are dispersed throughout the ST and within the more proximal region marked by *Tbx18*-expressing cells (Fig. 11G-I). *Hand1*-lineage cells are observed throughout the PE, consistent with a model where progenitor cells of the PE originate from the population of *Hand1*-expressing cells of the ST.

Hand2 is expressed during epicardiogenesis and is required for function of the epicardium

A surprising observation of the *Hand1* lineage analyses is the link established between the *Hand1*-lineage and the forming epicardium. As many epicardially deficient mouse models correlate with the time of death observed in *H2CKOs, Hand2* ISH were performed at E9.5 and E10.5 to assess *Hand2* expression within the epicardial lineage (Fig. 12A,B,E,F) (Moore et al., 1999).

Indeed *Hand2* expression is robust throughout the PE. *Hand2* is also expressed within epicardial cells at E10.5 as well as in isolated epicardial cells (arrow, Fig. 12E, Fig. 13). *Hand2* expression is not detected in *H2CKOs* within the epicardium or the PE, confirming that the *Hand1*-positive cells within the early ST populates the PE and epicardium. Together this shows novel expression of *Hand2* within the epicardium and a potential hierarchical relationship between *Hand1* and *Hand2* within establishing the epicardium.

To determine if *H2CKOs* have epicardial defects, we performed histological analysis at E14.5 (Fig. 12I,J). E14.5 Transverse sections revealed abnormal compaction and the absence of epicardium in conjunction with a lack of blood filled lumens running thru the epicardium, indicating epicardial phenotype for *H2CKOs* (Fig. 12I-J). Analysis of epicardial markers at E10.5 (data not shown) and E12.5 *ISH* for *Tcf21* suggests that the specification and formation of the early epicardium occurs normally (Fig. 12C,D). To determine whether the impact on epicardial development was a direct result of Hand2 function within the epicardium, we performed a conditional knockout of *Hand2* within the *WT1* lineage utilizing the $WT1^{ERT2Cre}$ mouse line (Zhou et al.) (Fig. 12G,H,K,L). At E13.5, $Hand2^{fx/-}$;*WT1-Cre* mutant embryos display a poorly organized epicardium compared to *WT* embryos, and display a visible reduction in *WT1*-lineage marked cells(Fig. 12K-L), and appear to phenocopy the epicardial defects observed within *H2CKOs*. These two independent epicardial Hand2 ablations indicate that *Hand2* is not necessary for the initial establishment of the

epicardium but rather plays a role in maintenance, differentiation, and function of the maturing epicardium.

Hand2 is required for the cardiac fibroblast fate and maintenance of coronary vasculature

Since *Hand2* loss-of-function leads to epicardial defects, we sought to further identify the role for *Hand2* in the epicardium. Platelet Derived Growth Factor (PDGF*)* receptors have been shown to play an essential role in cell fate and specification of the mature epicardium (Mellgren et al., 2008; Tallquist and Kazlauskas, 2004; Tallquist and Soriano, 2003). *ISH* for *PDGFR*α at E12.5 indicate a decrease in *PDGFR*α *e*xpression in the epicardium (Fig. 14A,B). To look at the potential impact on epicardially-derived cardiac myofibroblasts, ISH for *Periostin* (*Postn)*, a marker of the cardiac fibroblast cell fate, shows a marked decrease in *Postn*-positive cells invading the myocardium of E12.5 *H2CKO* mutant hearts (Fig. 14C-D) (Snider et al., 2008). The decrease in *Postn*-positive cells within the myocardium suggests that *Hand2* may play a role in determining epicardial cell fates that specify after epicardial cells undergo secondary EMT.

Due to the observation that *H2CKOs* lacked blood filled lumen on the surface of the heart, we performed Flk1 immunohistochemistry at E12.5 to determine if there were any defects in coronary vessel formation (Shalaby et al., 1995) (Fig. 14E-F). Immunohistochemistry indicates an absence of Flk1-positive cells running thru the epicardium. Counterstaining with Phalloidin shows that the epicardium is still intact, though absent of potential Flk1 lumens. Previous

studies have shown the epicardium does not give rise to coronary vasculature and the *Hand1*-lineage does not contribute to this endothelial cell population (Barnes submitted) (Red-Horse et al., 2010). Therefore, the severe abnormalities within the coronary vasculature of *H2CKOs* are likely due to non-cell autonomous mechanisms that involve cell-cell communication between coronary endothelium and the contributing epicardial-derived smooth muscle

To confirm that *H2cKO* coronary defects are secondary to epicardial defects, when conditional ablated using $Hand1^{Cre}$ and not resulting from *Hand2* ablation from myocardium or NCC (Fig. 14G,I,K), we generated *H2cKOs* $Wt1^{Cre}$, and employed immunohistochemistry for Cre-lineage and Flk1 (Fig. 14H,J,L). WT1-lineage results confirm that the epicardium does not contribute to coronary vasculature in phenotypically wild type mice. However, in *WT1*-genereatated *H2cKOs*, coronary lumens could not be detected thus confirming the non-cell autonomous affects of the *Hand2*-deficient epicardium.

To further address the impaired function of *H2CKO* epicardium, we generated Epicardial Primary Cultures (EPCs) from wild type and *H2CKOs* and isolated total RNA for microarray expression comparison. Gene ontology from our microarray analysis indicates significant differences between developmental and functional programs within the EPCs (Fig. 14M). Quantitative RTPCR on EPCs in WT and *H2CKOs* was performed to validate observed changes in gene expression levels observed in the microarray (Fig. 14N). Quantitative RTPCR confirms expression of *Hand2* within the epicardium as well as its ablation in the *H2CKO* EPCs. Interestingly results confirm that the ratio of *PDGFR*α*:PDGFR*β is

greatly altered in *H2cKO* EPCs. Expression of *PDGFR*α is significantly reduced whereas *PDGFR*β is significantly upregulated. PDGFRβ-mediated signaling is associated in promoting the smooth muscle fate from the epicardium while a role for PDGFRα signaling in influencing epicardial cell fate is currently unclear (Mellgren et al., 2008). The observed decrease in the detection of *Postn*-positive myofibroblasts within the compact zone of the heart, suggests that *PDGFR*α may impact fibroblast differentiation from the epicardium progenitors. Together, this suggests that *Hand2* directly impacts cell fate thru a potential *PDGFR*-dependent mechanism.

Hand2 **is required for proper** ***Fn1*** **fibril assembly, organization, and cell adhesion required functions**

As H2cKO epicardial defects appear direct, we then looked at the impact upon epicardial mesothelium integrity. *Fn1* has been shown to be downregulated in *Hand2* mutants (Trinh et al., 2005). Fn1 fibril assembly can regulate the organization and stability of ECM protein, is capable of promoting EMT and adhesion dependent growth, and defects in *Fn1* underlie integrin mediated valve leaflet defects in the lymphatic system and is associated with cell signaling via integrins (Bazigou et al., 2009; Kadler et al., 2008; Leiss et al., 2008; Liao et al., 2002; Sottile et al., 1998). Immunohistochemistry for Fn1 at E12.5 shows that Fn1 is expressed in the epicardium and is neatly organized around developing coronary vessels (Fig. 15A). *H2CKOs* retained Fn1 in the epicardium, however it appears unorganized (Fig. 15B). To obtain a more detailed look at Fn1 organization, we compared EPCs from wild type and H2cKOs (Fig. 15C-F). From

examination of the epicardium in culture, it is obvious that Fn1 fibril assembly is compromised. Compared to wild type immunostaining where an organized lattes of Fn fibrils is evident, *H2cKO* reveals a disorganized distribution Fn1 throughout the cell where deposition is uniform and sheet-like (Fig. 15C-F). Fn1 dysfunction suggests a critical role for Hand2 in regulating the components of ECM assembly and directly impacting epicardium homeostasis during development. Alcian Blue staining was performed to verify an increase in ECM (Fig. 15G,H). Indeed, there appears to be an increase in Alcian Blue staining, suggesting there is an increase in ECM deposition.

Since Fn1 function is compromised in *H2CKOs* other extra cellular matrix components were analyzed. Gene ontology from microarray analysis to identify enriched biological processes indicates an enrichment in ECM based processes, such as cell-cell signaling, assembly, connective tissue development, and motility (Fig. 15I). Quantitative RTPCR on EPCs in WT and *H2CKOs* was done to look at alterations in *Fn1* expression levels (Fig. 15J). *Fn1* expression was fond to be unchanged, as has been previously reported (Yin et al., 2010).

In addition to its role as an ECM component, Fn1 promotes intracellular signaling via interactions with cell surface integrins (Ieda et al., 2009). To see if the observed Fn1 disorganization in *H2cKOs* potentially altered cell signaling, we looked at *integrin* expression by quantitative RTPCR (Fig. 15J). Indeed, expression of fibronectin receptor *ITGA4* is significantly upregulated within the *H2cKO* cultures suggesting a feedback response resulting from diminished

signaling. In contrast, *ITGA5* and *ITGB1* that do not convey Fn1-mediated signaling show no significant changes in expression.

Gene ontology data from microarray analysis also indicates enrichment for cell cycle regulation. Loss-of-function of *Hand2* has been implicated in the apoptosis of other cell types (Thomas et al., 1998). Additionally, increased abnormal ECM organization and deposition have been implicated in cell death (Frisch and Francis, 1994). Immunohistochemistry was performed for activated-Caspase3 and Phoso-Histone H3 at E12.5 to look at cell death and cell cycle in the epicardium of *H2CKOs* (Fig 15 K,L). No change is observed in proliferation, suggesting that the process of epicardial EMT is not affected (Wu et al., 2010). Interestingly, we observe an increase in cell death within the epicardium of the *H2CKOs*. This indicates that impaired ECM function in *H2CKO* may intricately be tied to not only proper function and integrity but also cell survival.

Chapter Three

Discussion

bHLH proteins depend upon dimer formation to bind DNA and regulate gene expression; thus, defining where these factors are expressed is necessary to evaluate their mechanistic roles during organogenesis. The dynamic spatiotemporal expression of Twist family bHLH proteins renders an understanding of their mechanistic and functional roles as dictated by dimer partner choices a significant challenge. Although loss-of-function analyses in both systemic and conditional models have provided insights into the role of Hand1 in extra embryonic, cardiac, and NCC derived tissues, the expression data available is still limiting.

Here, we have created a *Hand1* allele that permanently marks all *Hand1*-expressing cells, enabling their developmental fates to be monitored. In some instances, such as in extra embryonic structures, observations of the *Hand1*-lineage completely correlate with real-time expression; however, observations of lineage-marked cells clearly refine and expand real-time expression data, revealing novel potential domains of *Hand1* function. This is exemplified in the developing myocardium by the near exclusive restriction of *Hand1*-marked cells to ventricular structures derived from the FHF. The *Hand1*-lineage marks the outer curvature of the left ventricle, is absent from the atria, and is not expressed at significant levels within the SHF-derived right ventricle, which robustly expresses the related factor *Hand2*. As *Hand1* expression in the FHF

myocardium expands, *Hand2* expression dominates within the SHF cells that are migrating into the heart from both atrial and venous poles. *Hand1* is clearly expressed and specifically marks the SHF-derived myocardium within the myocardial cuff, a tight ring of myocardium in direct contact with the forming OFT. The *Hand1*-lineage does not contribute to the endocardium, whereas *Hand2* is expressed within these cells. Therefore, *Hand1* and *Hand2* expression overlaps within FHF derived myocardium of the left ventricle beginning at E8.5 and within the SHF derived myocardial cuff at E9.5. Expression within other SHF-derived myocardium and endocardium is exclusively defined by *Hand2*.

The *Hand1*-lineage analyses potentially reveal a novel role for Hand1 in the formation of the epicardium. Comparison of $Hand1^{LacZ/+}$ and $Hand1^{eGFPCre/+}$ mice up to E9.5 shows no significant variation within the forming heart. By E10.5, the entire surface of the heart is composed of *Hand1*-lineage marked cells, whereas real time *Hand1* expression is not observed. We also observed that coronary smooth muscle and cardiac fibroblasts, but not coronary endothelium, are derived from *Hand1*-expressing cells. Given that the epicardium gives rise to both cardiac fibroblasts and the smooth muscle of the coronaries, but not coronary endothelium, this supports the conclusion made by Red-Horse et al., that coronary endothelium is not a derivative of the epicardium, but comes from endothelial progenitors within the sinus venosae. Exploring the role Hand1 plays in defining epicardial progenitors will be an interesting and informative area to pursue.

In addition to expression in the heart, *Hand1*-lineage contributes to the cardiac OFT, jaw, sympathetic nervous system and lateral mesodermal derivatives of the gut. Within the OFT, *Hand1*-lineage analysis suggests that the majority of cNCC within the OFT, at some point in their emigration, expressed *Hand1*; however, real-time expression at E10.5 shows that only a subset (approximately 50%; (Vincentz et al., 2008) actively express *Hand1* transcript. These cNCC are interesting in that they coexpress *Twist1* and *Hand2*, and although deletion of *Hand1* in the NCC via *Wnt1-Cre* is reported to show no obvious OFT phenotypes (Barbosa et al., 2007), the *Hand1 and Hand2* real-time expressing cells are observed to selectively show defective cell adhesion on the *Twist1* null background (Vincentz et al., 2008). Given that gene dosage relationships between these potential dimer partners are evident, looking at more compound relationships between these factors using the *Hand1* eGFP-Cre driver could be informative.

In the sympathetic ganglia, *Hand1* expression is observed as early as E11.5. *Hand2* expression precedes this upregulation. *Wnt1-Cre* mediated *Hand2* deletion results in a loss of *Hand1* expression (Morikawa et al., 2007). *Hand1* expression within the sympathetic ganglia persists into adulthood and we observe no significant differences between real-time and *Hand1*-lineage expression patterns. Similarly *Hand1*-lineage analysis of the enteric nervous system does not show deviation from that of real-time *Hand1* expression.

Within the cranial NCC, Hand1, in conjunction with dosage modifiers such as Hand2, impairs growth of the distal midline mesenchyme (Barbosa et al.,

2007). Real-time *Hand1* expression marks the midline of the developing mandible and the midline of the tongue. The *Hand1*-lineage clearly marks the midline mesenchyme of the frontal processes of the face throughout all Meckel's cartilage derivatives. Additionally, the *Hand1*-lineage appears to contribute to a more extensive domain in the midline region of the tongue. This suggests that either *Hand1* expression becomes restricted during the differentiation process of the midline cranial neural crest cells or that the *Hand1*-lineage migrates outward from the site of active *Hand1* expression in the midline cranial neural crest.

Ectopic expression of Hand factors within the limb results in preaxial polydactyly (Fernandez-Teran et al., 2000; McFadden et al., 2002 Fernandez-Teran, 2003). Mechanistically, this phenotype is also a consequence of *Hand*/*Twist* gene dosage, where functional antagonism between Twist1 and Hand proteins mediated by dimer partner choice causes a variety of limb abnormalities (Firulli et al., 2005; Firulli et al., 2007). Real-time expression of *Hand1* within the mouse limb is restricted to the anterior-ventral area of mesoderm at mid-level in the proximo-distal axis (Fernandez-Teran et al., 2003). In chick, this expression is accompanied by expression within the ventral lateral mesoderm of the forming limbs, but this domain was not detected in the mouse. Interestingly, *Hand1*-lineage analysis defines forelimb vs. hindlimb differences. Forelimb *Hand1*-lineage expression appears to mirror real-time expression, with the exception that the increased sensitivity of the R26R reporter reveals *Hand1*-activty within the ventral mesoderm of the forming forelimb. The *Hand1* forelimb lineage experiment reveals the early contributions of *Hand1* expressing lateral

mesoderm to help establish dorso-ventral patterning (Johnson and Tabin, 1997). Molecularly, dorso-ventral patterning is established as an essential modular cascade within limb patterning and hobbling of this cascade models clinical limb defects (Ahn et al., 2001; Chen and Johnson, 2002; Chen et al., 1998; Grieshammer et al., 1996). Hindlimb contributions appear much more extensive than those revealed by real-time analyses and likely reflect the lateral mesodermal origin of the hindlimb mesenchyme. Although Hand1 function within the limbs is not well established, especially when compared to its putative dimer partners *Hand2* and Twist, the differential activity of this *Cre* allele could help define its role in limb morphogenesis.

The last and perhaps most important role for Hand1 is its functions in extra embryonic tissues and its role in the specification and differentiation of trophoblast giant cells (Firulli et al., 1998; Morikawa and Cserjesi, 2004; Riley et al., 1998). *Hand1* is persistently expressed in these extra embryonic tissues and trophoblasts cells and thus the *Hand1*-lineage does not add any additional insight. This expression raises the largest caveat with this *Cre*-driver in that, if extra embryonic expression is encountered, this *Cre* driver line would not be optimal for use in looking at gene ablation in embryonic structures. That being said, if potential targets for conditional deletion within the embryo are expressed in primary myocardium, post-migratory neural crest, lateral mesoderm and or hindlimb mesenchyme, use of this reagent could prove useful in dissecting mechanism via the conditional loss-of-function approach.

Together, the lineage and the conditional knock out data reveals a novel function for Hand factors in epicardiogenesis. Using Hand1-lineage data from our targeted Cre knockin, we present a model where transient expression of *Hand1* within the ST marks cells that go on to populate the PE and subsequently epicardium and its derivates. Directly downstream of *Hand1*, is the upregulation of *Hand2* within the PE, which when ablated results in significant epicardial lineage defects that result in persistent expression of *WT1* within migrating epicardial cells post secondary EMT, an impairment fibroblast differentiation, abnormal Fn1 deposition and organization associated with altered signaling, and an increased cell death. Collectively this results in poor functional integrity of the epicardium leading to a decline in epicardial function and a failure to form a patent coronary vasculature. The lack of epicardial function is likely the cause of death correlating well with other mouse models that show coronary malformations (Moore et al., 1999).

Fn1 is a multifunctional protein helping to establish cytoskeletal organization, motility, and cell signaling pathways involved in proliferation and growth. As epicardial cells must migrate, alter morphology, and ultimately differentiate into functional cell type, the epicardial phenotypes observed in *H2CKOs* mechanistically are all dependent on Fn1 function. Fn1 and ITGA4, a Fn1-specific receptor expressed within the epicardium, have been implicated in phenotypes associated with similar mesodermal, epicardial, and cardiovascular decline (George et al., 1997; George et al., 1993; Georges-Labouesse et al., 1996; Yang et al., 1995). Additionally, alterations in Fn1 deposition are

associated with an increase in fibrosis and cell death (Tomita et al., 2007), phenotypes, which are observed in the *H2CKO* epicardium. Interestingly the functional regulation of Fn1 by Hand2 is clearly indirect in that mRNA and overall levels of FN1 protein not significantly altered in H2cKO epicardium. This suggests that additional ECM proteins, which are Hand2-dependent directly, influence Fn1 organization and deposition. *Hand2* has been previously associated in regulating Fn1 deposition and has more recently been revealed to influence ECM deposition during lateral mesoderm remodeling prior to midgestation in zebrafish (Trinh et al., 2005). Our data is completely consistent with these observations indicating that this functional role is not only evolutionarily conserved but also critical for maturation of epicardial derived cell types that clearly influence both myocardium and coronary endothelium non-cell autonomously.

We observed no *Hand1*-lineage endothelial cells contributing to the coronary vessels within wild type or H2cKO mice. The origin of the coronary vessels endothelium is currently understood to be the sinus venosus (Red-Horse et al., 2010), and it is presumed that a functional epicardium is required for establishing and maintaining the patency of the coronary vessels. *H2CKOs* appear to have lineage specific defects that impact both fibroblast and smooth muscle cell fates of the epicardium post secondary EMT. Close examination of *Hand1*-marked epicardium does not indicate the presence of *Hand1*-lineage independent cells (Barnes Submitted); moreover, *Hand2* ISH similarly marks the entire epicardium suggesting that *Hand2* is not enriched within a specific

epicardial lineage. Previous work establishes a relationship for PDGFRs to govern specific lineage subsets during epicardial development (Mellgren et al., 2008; Tallquist and Kazlauskas, 2004). PDGFRα is downregulated within *H2CKO* epicardium. Although a role for *PDGFR*α has not been clarified within the epicardium, it has been shown to be essential in other EMT derived cell populations (Tallquist and Soriano, 2003). Interestingly, PDGFRβ is reciprocally upregulated within *H2CKO* epicardium. This change in ratio between these related receptors could simply be the result simple compensation of *PDGFR*β for the decreased expression of *PDGFR*α; however, PDGFRβ function has been directly associated with driving smooth muscle cell fates from epicardial derived cell populations (Mellgren et al., 2008). Given epicardium gives rise to both fibroblast and coronary smooth muscle and we observe a reduction in fibroblast invading the myocardium (Fig. 6), this may indicate an essential role for PDGFRα in governing the fibroblast fate (Richarte et al., 2007) and that modulating the ratio of PDGFRs that govern these divergent cell programs is Hand2-dependent developmental program.

In addition to the phenotypes observed within the epicardial lineage, Hand2 defects are observed within the cardiac OFT. Wnt1-Cre NCC specific deletion of *Hand2* reports arch defects, DORV, and associated VSDs (Holler et al., 2010). Considering that *Hand2* ablation within the *Hand1*-epxressing cNCCs is temporally delayed and spatially more restricted then *Hand2*$^{\Delta NCC}$, the high penetrance of a more severe NCC-dependent PTA phenotype suggests that genetic and possibly functional interactions between Hand1 and Hand2 are

critical for OFT septation as *H2CKOs* generated using *Hand1*^{Cre} are heterozygous null for *Hand1*. These data are supported by the previously identified genetic interactions between *Hand1* and *Hand2* within the left ventricular myocardium and the pharyngeal arches (Barbosa et al., 2007; McFadden et al., 2000) and is directly supported with established dimer regulation mechanisms that govern the dimer formation and biological output of Twist-family bHLH factors. Indeed dysregulation of Twist1 dimerization is causative of the autosomal dominant human disease Saethre Chotzen Syndrome and directly reflects molecular antagonism between Twist1 and Hand2 (Firulli et al., 2005; Jabs, 2004). The idea that Hand1 and Hand2 dimer choice is modulated by phosphoregulation and/or gene dosage/expression dictates a well-supported biological model for Hand factor function in OFT morphogenesis and experiments to investigate the latter mechanism are currently underway.

A final observation is that *Hand1* and *Hand2* display very unique expression domains within the developing murine heart. *Hand1* is largely restricted to the cells of PHF that make up the left ventricle and expression within the SHF is restricted to the myocardial cuff that makes direct contact with the NCC-derived OFT (Barnes, submitted). It is this SHF domain where co-expression with *Hand2* is visibly persistent. *Hand1* expression and lineage is detectable at E8.5 within the forming left ventricle and it is at this stage, during the onset of cardiac looping. Although we observe a thin compact zone and hypertrabeculation within *H2CKOs,* the cell autonomy of these defects cannot be deduced. *Hand2* ablation using cardiac a specific Cre results in early embryonic

death exhibiting a similar phenotype to the systemic Hand2 knockouts suggesting that these defects are SHF-dependent (Morikawa and Cserjesi, 2008). Although *Hand1*^{Cre} mice allow insight into a possible role for Hand2 in the PFH myocardium, isolation of the PHF enhancer or use of a PHF-specific Cre will be required to address this directly. Collectively, these studies demonstrate, that in addition to the established roles of Hand2 within the cNCC and myocardium, Hand2 plays a novel and critical role in the function and differentiation of epicardium, by modulating cell signaling mechanisms that dictate epicardial cell fates as well as ECM organization that is required for proper formation and function of the heart.

Overview & Future Aims

The *Hand1* lineage has provided substantial descriptive and mechanistic insight into Hand factor function. Analyzing the *Hand1* lineage was a daunting task given the dynamic spatial and temporal expression domain. However, the lineage analysis proved to be insightful into highly specific contributions to different developmental lineages. This descriptive data suggests further insight into the neccessity and function of *Hand1* throughout development. Additionally, given the dynamics and promiscuity of Hand factor dimer pairing, the *Hand1* lineage analysis focuses our insight into Hand protein distribution and dimer regulation.

Descriptive analysis of the *Hand1* lineage led to spatial clarification for *Hand1* in several lineages. Strikingly, the *Hand1* lineage contributed to vascular endothelium in multiple developmental spatial systems throughout the embryo. *Hand1* has not been documented as previously being expressed in vascular endothelium. Vascular endothelium of the descending dorsal aorta raises questions about lateral mesodermal precursors in which *Hand1* is actively expressed. Additionally, lineage analysis for *Hand1* in the placental labyrinth vascular endothelium proposes a novel role for *Hand1* during labyrinth development and possibly creating a more complex role for *Hand1* during placental development. The analysis of limb lineage data reveals a surprising early contribution of *Hand1*-positive cells to the limb buds in addition to a specific localization within the A-P axis of the developing forelimb. Lineage analysis also

illustrates an expansion in the contribution for *Hand1* within the mesothelial cell population, given the insight derived from epicardial cell derivatives. NCC analysis revealed a striking refinement in postmigratory NCC for the *Hand1* lineage and suggests highly specific function for *Hand1* in this population. Finally, the *Hand1* lineage allowed a conclusive examination of *Hand1* function during left ventricular development and provides much needed discussion for this pivotoal chamber and tissue specific transcription factor since the onset of heart lineage data reconstructed our models for cardiogenesis.

The result of the *Hand1* lineage analysis raises many questions that may be addressed in future studies. Conditional ablation studies using vascular specific *Cre Recombinase* mouse lines may offer insight into the functional roles for *Hand1* in both dorsal aorta and placental labyrinth function. Cell surface marker profiling of *Hand1*-positive erythrocytes via FACS analysis and colony forming unit experiments may lead to exciting subset profile that may implicate the *Hand1*-lineage in endothelial stem cell development. The derivatives of *Hand1*-expressing cells in the septum transversum may lead to multiple projects in the near future. First, a loss-of-function experiment for *Hand1* may implicate it mechanistically in defining mesothelial precursors. Second, functional implication may be further enhanced by the identification of a novel enhancer element. Finally, a transgenic *Cre Recombinase* mouse line following the potential discovery of a septum transversum specific enhancer would be a highly sought

after tool by the scientific community due to the lack of a true epicardial cre line to this point.

Conditional ablation experiments utilizing the *Hand1*^{Cre} to ablate *Hand2* have led to substantial insight into Hand factors dynamics and functional overlap during development. The lineage assessment of *Hand1* led to a rigorous examination of Hand factor expression during cardiogenesis. This resulted in redefining *Hand* factor expression as more distinct than previously reported. Thought the factors are complex in terms of function, these experiments confirm they do not appear to be functionally redundant using a loss of function model. While *Hand2* has been implicated primarily as a NCC and mesodermal transcription factor, the results from this study reveals unique insight for *Hand2* in mesothelial cardiac populations while expanding mechanistic insight for *Hand2* in cell survival, matrix organization, and cell fate selection.

These loss of function experiments suggest future experimental studies in the near future. Although the study entails several conditional *Cre Recombinase* mouse lines, the conditional ablation of *Hand2* in the epicardium has been hampered due to difficulties in finding *Cre* mouse lines that are truly restricted to epicardial mesothelium. Either development of other more specific epicardial *Cre* drivers or the development of a *Hand1* septum transversum cre line would enable a more tailored examination of *Hand2* epicardial deletion. Given the specific role for *Hand1* in mesothelial and vascular labyrinth placental populations, and given the close temporal expression between Hand factors, it might prove useful to

scrutinize placental expression of *Hand2* and identify suitable *Cre Recombinase* mouse lines that would test an expanded role for *Hand2* during placental development. Insight into modulation of epicardial cell fate effectors was novel to the *Hand2* literature. Unfortunately, the tools in these studies were insufficient to thoroughly assay the impact of *Hand2* on cell fate. Utilizing *Hand2* expression and siRNA adenovirus on ES cells bearing transgenic eGFP reporters for *Thy1*, *Myh11*, *Wt1* may yield further insight into epicardial fate. The enlightenment of *Hand2* expression in cardiovascular lineages raises the ideas to pursue a more thorough cardiac chamber study. Generating a $Hand2^{LacZ}$ allele would be an essential tool for expression analysis. Additionally, utilizing SHF *Cre* mouse lines in conjunction with utilizing *Hand2* expression and siRNA adenovirus' on ES cells bearing transgenic eGFP reporters would enhance our understand of the function of this essential and highly evolutionarily conserved bHLH protein.

Chapter Four

Figures

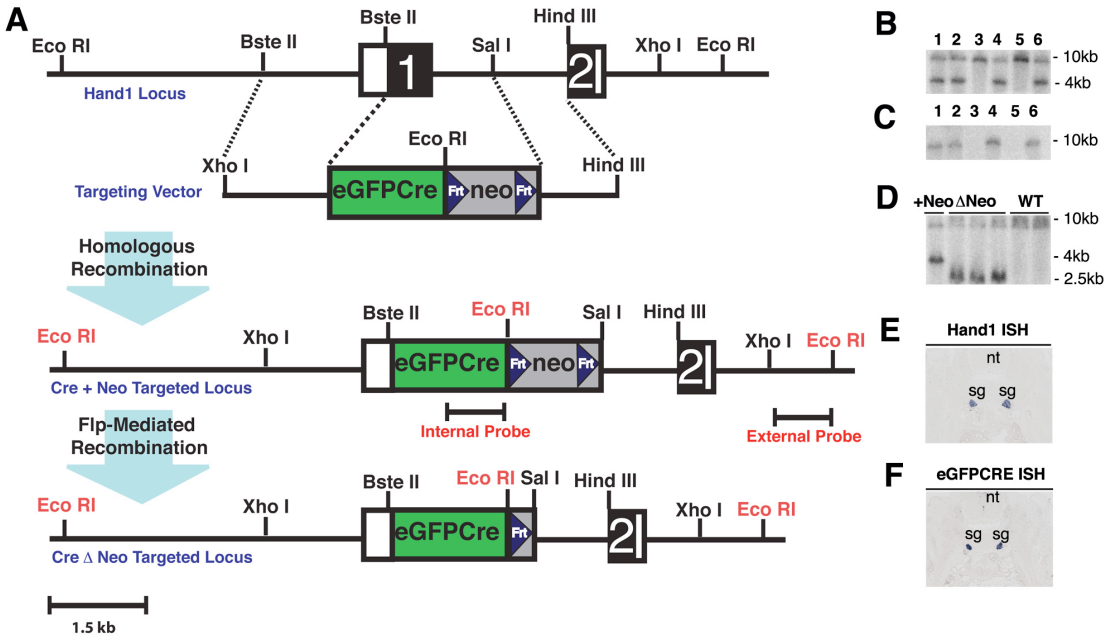

Figure 1: Generation and validation of the *Hand1*^{eGFPCre} mouse line. A) The *Hand1* locus is shown at the top with non-coding and coding regions indicated by the white and numbered-black boxes, respectively. The targeting vector is shown below with the dotted lines indicating regions of sequence identity between the targeting arms. The targeting strategy introduced an *eGFPCre* cassette into the 5' untranslated region of *Hand1*, followed by an *FRT*-flanked *PGK-neo*. Homologous recombination resulted in deletion of the first exon of *Hand1* and insertion of the *eGFPCre* gene under control of the endogenous promoter. Following germline transmission of the mutation, the *PGK-neo* was deleted by subsequent mating with the *FLPeR* mouse line. B) Southern blot of

Hand1$^{eGFPCre+Neo/+}$ offspring using an external probe to detect the targeted allele and C) using an internal probe to confirm the absence of transgenic incorporation of the targeting construct. D) Southern blot of *Hand1*$^{eGFPCre\Delta Neo/+}$ offspring following *Flp Recombinase* mediated deletion of the *PGK-neo*. (E, F) RNA *in situ* hybridization on E13.5 *Hand1*$^{eGFPCre\Delta Neo/+}$ embryos shows identical tissue-specific *Hand1* and *eGFPCre* expression.

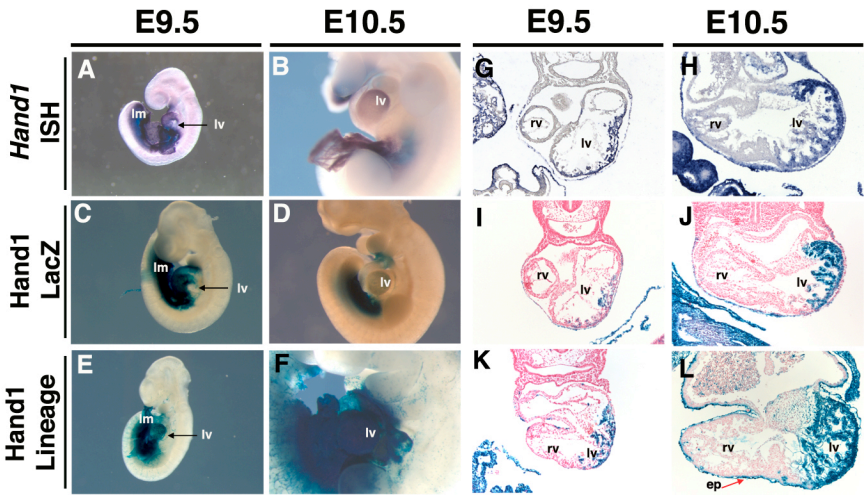

Figure 2: The *Hand1*-Lineage contributes to a subset of the first heart field and epicardium. DIG-labeled whole-mount (A, B) and transverse section (G, H) *in situ* hybridization for *Hand1* on wild-type embryos at E9.5 and E10.5. LacZ staining of the *Hand1*^{LacZ} (C, D, I, J) and *Hand1*^{eGFPCre} lineage (E, F, K, L). ep, epicardium; lm, lateral mesoderm; lv, left ventricle; rv, right ventricle.

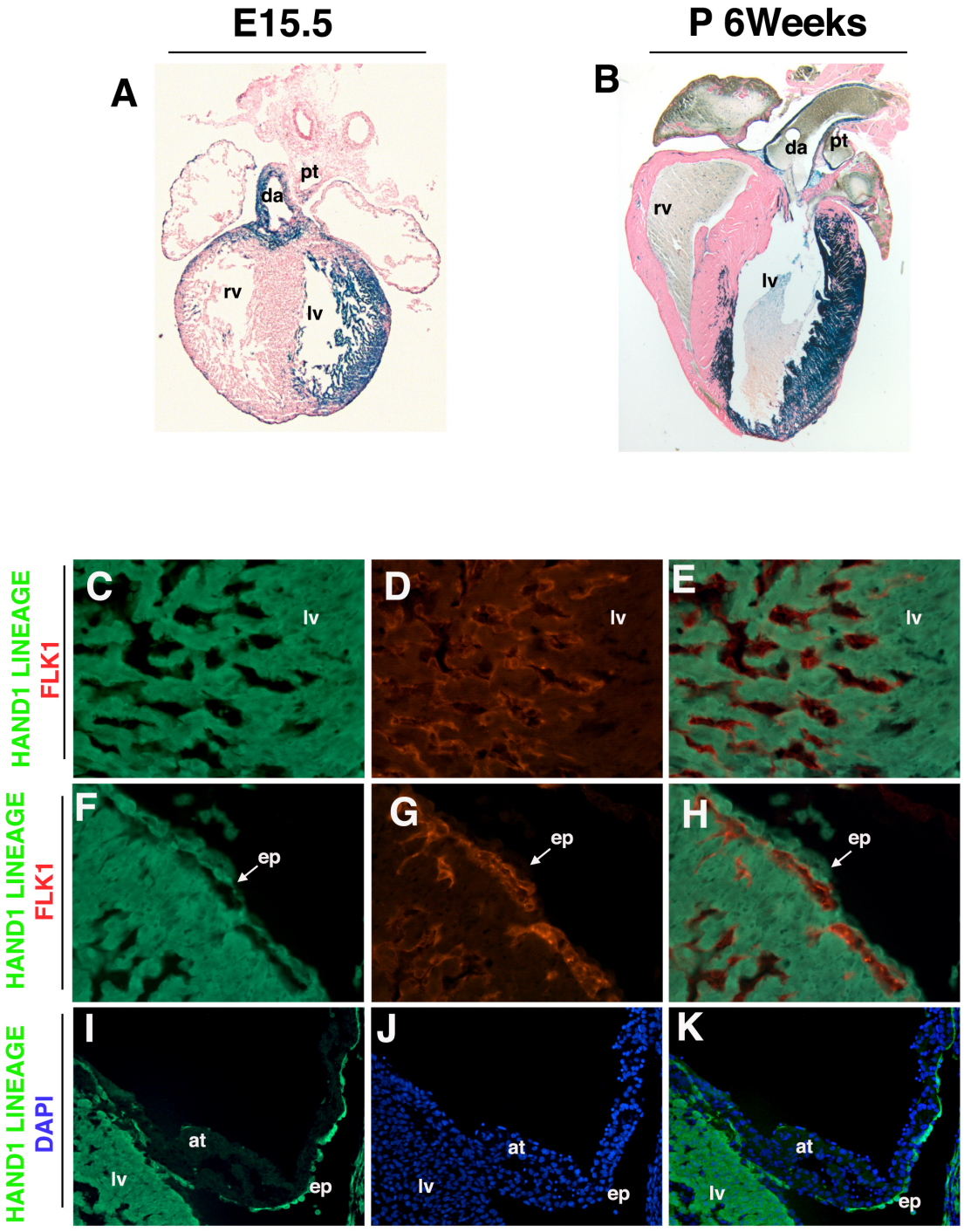

Figure 3: Analysis of the adult *Hand1* lineage shows restriction to specific cardiovascular lineage subsets. LacZ staining of *Hand1*-lineage cryosections

(A, B). E13.5 immunohistochemistry for Flk1 (red; D, G) and the *Hand1*-lineage (green; C, F). Overlay of Flk1 and the *Hand1*-lineage (E, H). E13.5 immunohistochemistry for the *Hand1*-lineage (green; I) counterstained with DAPI (blue; J). Overlay for DAPI and the *Hand1*-lineage (K). at, atria; da, dorsal aorta; ep, epicardium; lv, left ventricle; pt, pulmonary trunk; rv, right ventricle.

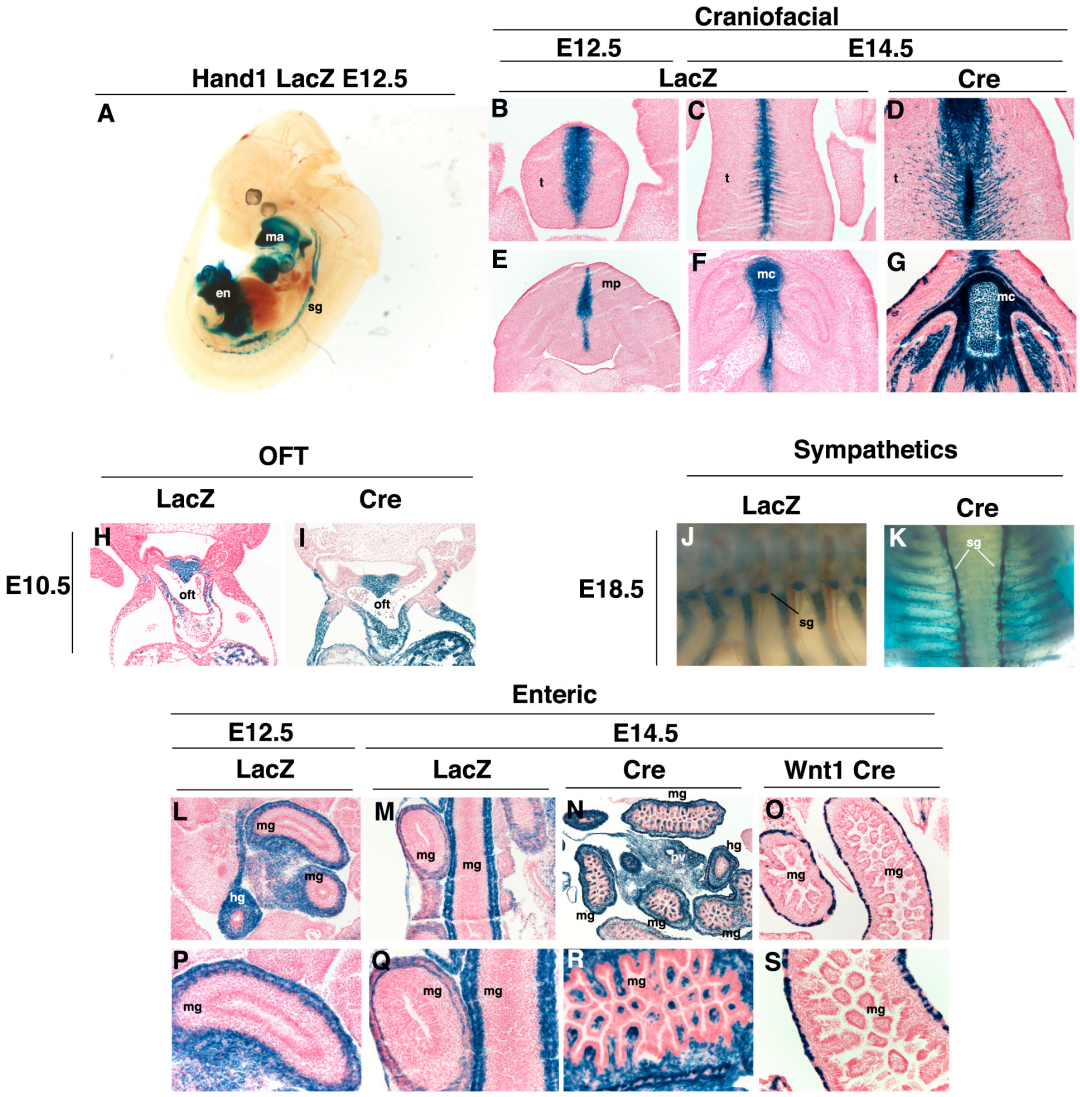

Figure 4: The *Hand1*-lineage marks discrete neural crest cell populations. Whole-mount LacZ staining of *Hand1*^{LacZ} (A,J) and the *Hand1*-lineage (K). Transverse sections of whole mount LacZ stained *Hand1*^{LacZ} (F) and *Hand1*-lineage (G) embryos. LacZ staining of *Hand1*^{LacZ} (B, C, E, F, L, M, P, and Q), *Hand1*-lineage (D, G, N, and R), and *Wnt1*-lineage (O,S) cryosections. en,

enteric; hg, hindgut; ma, mandible; mc, meckel's cartilage; mg, midgut; mp, mandibular process; oft, outflow tract; pv, posterior vein; sg, sympathetic ganglia; t, tongue.

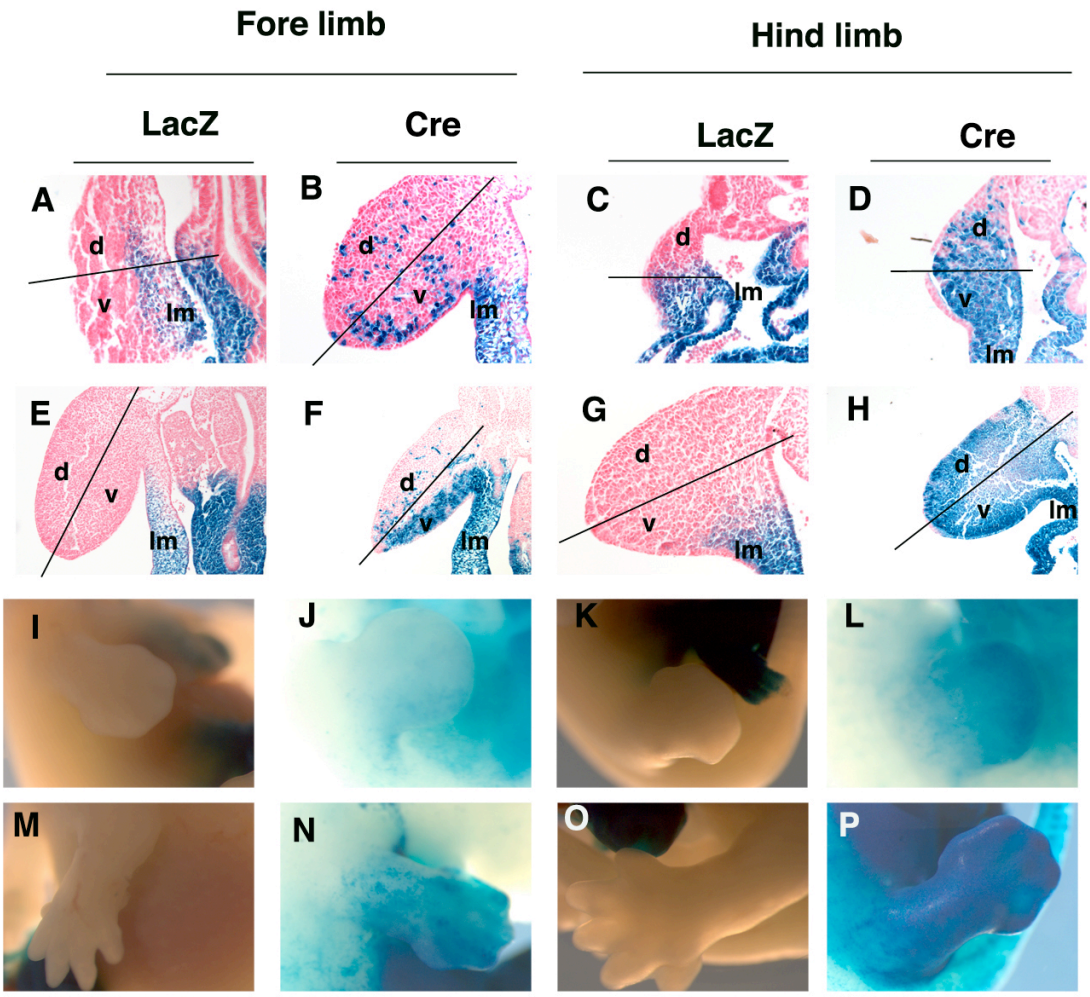

Figure 5: Analysis of the *Hand1* limb lineage. LacZ Staining of *Hand1*^{LacZ} and the *Hand1* lineage at E9.5 (A-D), E10.5 (E-H), E12.5 (I-L), and E14.5 (M-P). Transverse sections of LacZ stained embryos showing fore and hind limbs (A-H). Whole-mount LacZ staining (I-P). d, dorsal; lm, lateral mesoderm; v, ventral.

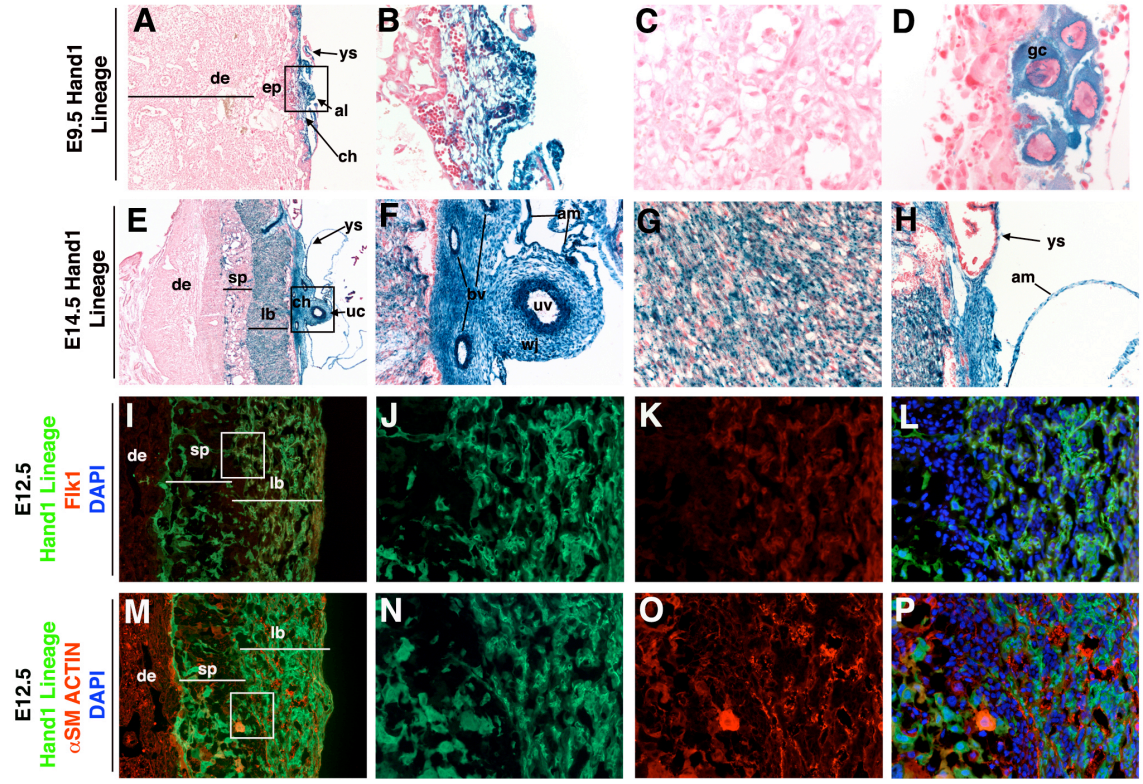

Figure 6: The *Hand1* lineage contributes to the EEM and Trophoblasts during placental development. LacZ staining of *Hand1*-lineage cryosections (A-H). Immunohistochemistry for the *Hand1*-lineage (green; I, J, M, N), Flk1 (red; K), αSM-Actin (red; O). Overlay for the *Hand1* lineage, Flk1, and DAPI (blue; L). Overlay for the *Hand1* lineage, and αSM-Actin, DAPI (blue; P). al, allantois; am, amnion; ch, chorion; de, decidua; ep, ectoplacental plate; gc, giant cell; lb, labyrinth; sp spongiotrophoblast; uc, umbilical chord; uv, umbilical vessels; ys, yolk sack; wj, Wharton's jelly.

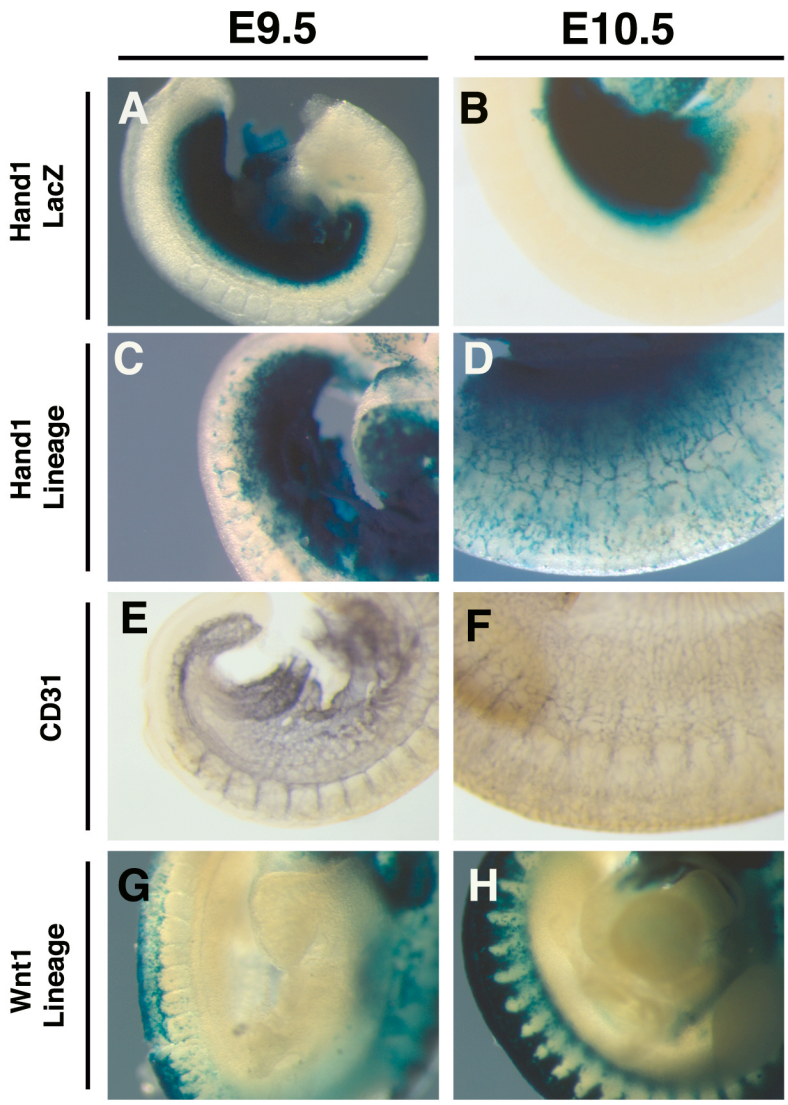

Figure 7: Lateral mesodermal derivatives of the *Hand1* lineage gives rise to intussuceptive microvascular growth. Whole-mount LacZ staining of the *Hand1*^{LacZ} (A, B), the *Hand1*-lineage (C, D), and the *Wnt1*-lineage (G, H). Whole-mount antibody staining for CD31 (E, F).

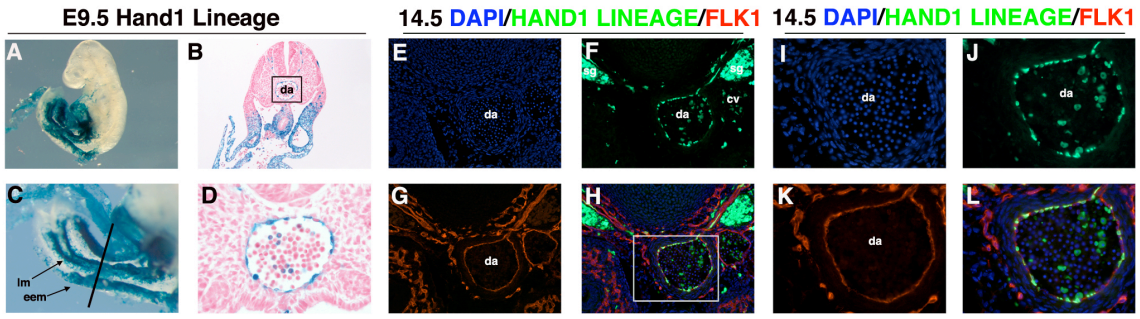

Figure 8: Lateral mesodermal derivatives of the *Hand1* lineage give rise to endothelial progenitors of the dorsal aorta. Whole-mount LacZ staining of the *Hand1*-lineage (A, C). Transverse sections of whole mount LacZ stained *Hand1*-lineage embryos (B, D). Immunohistochemistry for the *Hand1*-lineage (green; F, J), Flk1 (red; G, K), and DAPI nuclear staining (blue; E, I). Overlay for the *Hand1*-lineage, Flk1, and DAPI (H, L). cv, cardinal vein; da, dorsal aorta; eem, extra embryonic mesoderm; lm, lateral mesoderm; sg, sympathetic ganglia.

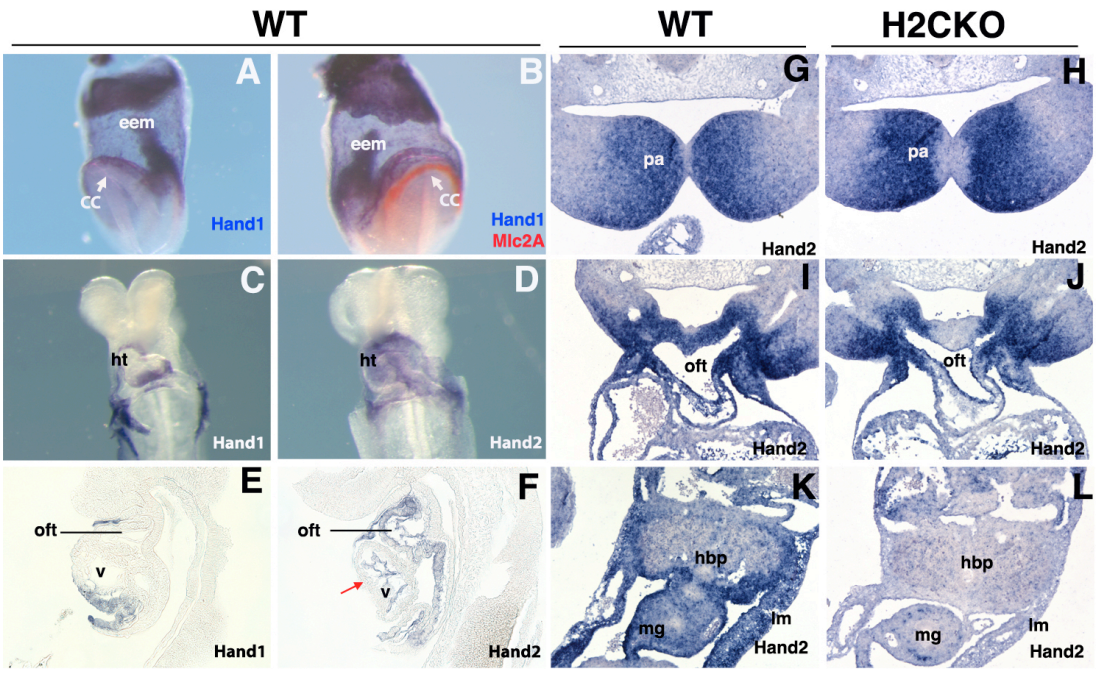

Figure 9: Inactivation of *Hand2* within the *Hand1* lineage. Single and double-labeled *Mlc2a* and *Hand1* whole mount RNA *ISH* of E7.5 embryos show that *Hand1* is not expressed within the cardiac crescent (white arrow) but is expressed within overlying extra embryonic mesoderm, allantoic rudiment, and the chorion (A,B). *Hand1* and *Hand2* whole mount RNA *ISH* of E8.5 embryos shows complimentary expression of Hand factors early during cardiac development (C-F). *Hand2* expression is confined to the SHF and endocardium of the developing ventricular chamber (black arrow). *Hand2* RNA *ISH* on transverse sections at E10.5 shows the deletion of *Hand2* within the *Hand1*

lineage (G-L). Deletion of *Hand2* is restricted to a distinct subset of NCC, cardiovascular, and lateral mesoderm derivatives where Hand factors are coexpressed. cc, cardiac crescent; eem, extra embryonic mesoderm; hbp, hepatic/biliary primordia; ht, heart tube; lm, lateral mesoderm; mg, midgut; oft, outflow tract; pa, pharyngeal arch; v, ventricle.

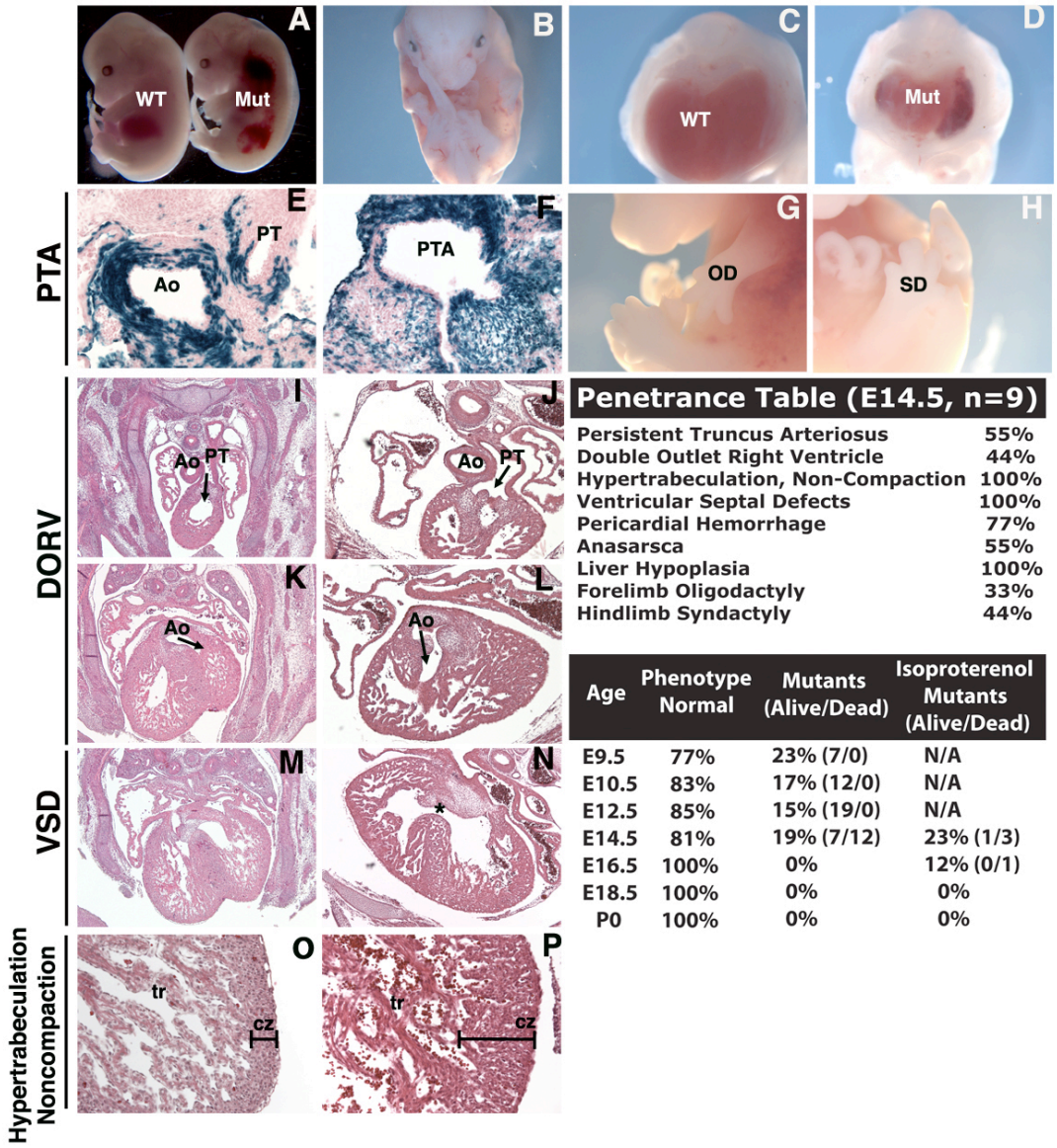

Penetrance Table (E14.5, n=9)	
Persistent Truncus Arteriosus	55%
Double Outlet Right Ventricle	44%
Hypertrabeculation, Non-Compaction	100%
Ventricular Septal Defects	100%
Pericardial Hemorrhage	77%
Anasarsca	55%
Liver Hypoplasia	100%
Forelimb Oligodactyly	33%
Hindlimb Syndactyly	44%

Age	Phenotype Normal	Mutants (Alive/Dead)	Isoproterenol Mutants (Alive/Dead)
E9.5	77%	23% (7/0)	N/A
E10.5	83%	17% (12/0)	N/A
E12.5	85%	15% (19/0)	N/A
E14.5	81%	19% (7/12)	23% (1/3)
E16.5	100%	0%	12% (0/1)
E18.5	100%	0%	0%
P0	100%	0%	0%

Figure 10: Conditional deletion of *Hand2* within the *Hand1* lineage results in extensive embryonic and cardiovascular defects. Whole mount (A-D, G, H) and histological (E, F, I-P) analysis of phenotypes in *H2CKO* embryos at E14.5. Mutant mice display pericardial hemorrhaging (A) and extensive edema, termed anasarca (B). Compared to WT mice (C), mutant mice have hypoplastic livers

with extensive hemorrhaging (D). Histological examination of embryonic hearts reveal extensive cardiovascular phenotypes. *H2CKOs* have both DORV and PTA's OFT defects (E-N). In the ventricles, *H2CKOs* exhibit full penetration of VSD's. Closer examination shows abnormal trabeculae and the absence of compaction in the compact zone (O,P). ao, dorsa aorta; cz, compact zone; od, oligodactyly; pt, pulmonary trunk; pta, persistent truncus arteriousus; sd, syndactyly; tr, trabeculae.

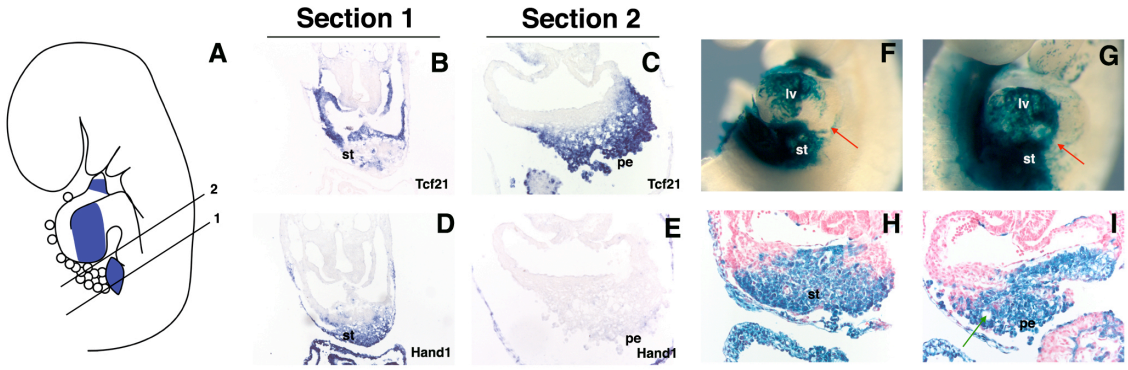

Figure 11: The *Hand1* lineage gives rise to epicardial progenitors. E9.5 cartoon illustrating *Hand1* expression (blue) and showing planes of section in B-E (A). *Hand1* and *Tbx18* section *ISH* of E9.5 embryos on adjacent sections through the septum transversum and the proepicardium (B-E). *A*nalysis shows that *Hand1* expression is not detected within the proepicardium but is expressed in the septum transversum. LacZ staining of both the *Hand1*^{LacZ} (F) and *R26R* activation via *Hand1*^{eGFPCre} *(G-I)* shows *Hand1*-lineage cells within the septum transversum and in the proepicardium, confirming that *Hand1* is expressed in proepicardial progenitors. lv, left ventricle; pe, proepicardium; st, septum transversum.

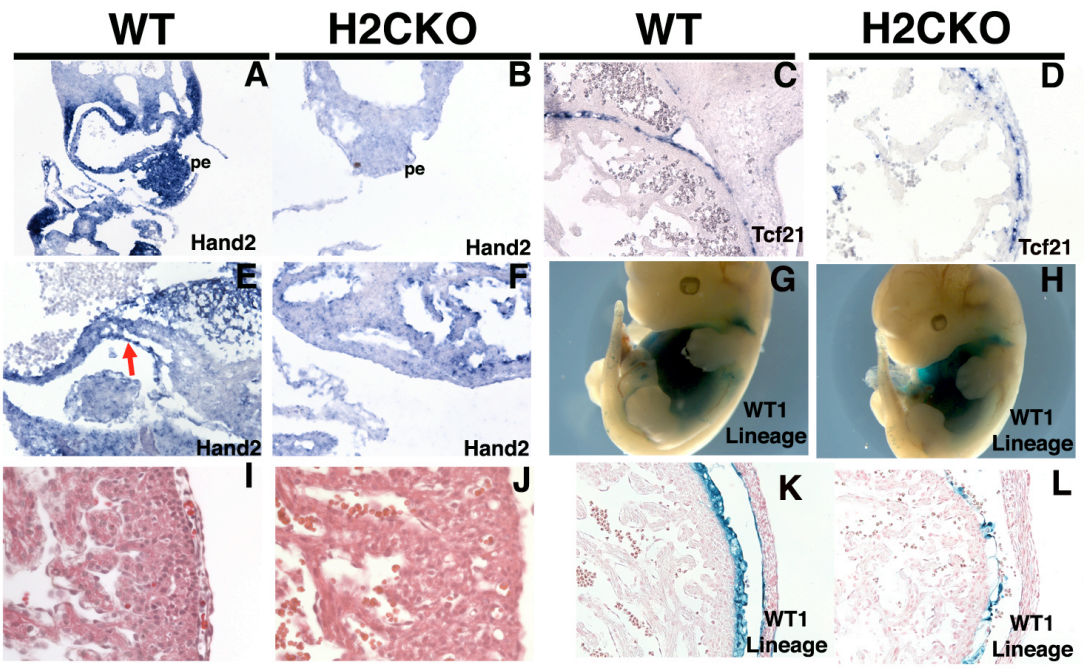

Figure 12: Loss of *Hand2* results in a lethal epicardial phenotype. RNA *ISH* at E9.5 (A-B) shows *Hand2* expression throughout the proepicardial organ and in the epicardium (red arrow) at E10.5 (E-F). Consequently, *Hand2* expression is ablated in the presumptive epicardial mesothelium in *H2CKOs*. Histological examination at E14.5 shows a lack of epicardium and compaction abnormalities in *H2CKOs* (I-J). RNA *ISH* for *Tcf21* at E12.5 shows normal establishment of the epicardium (C-D). LacZ staining and conditional deletion of *Hand2* within the *Wt1* lineage at E13.5 recapitulates epicardial defects and time of death observed in *H2CKOs* via *Hand1*^{eGFPCRE} (G-L). pe, proepicardium.

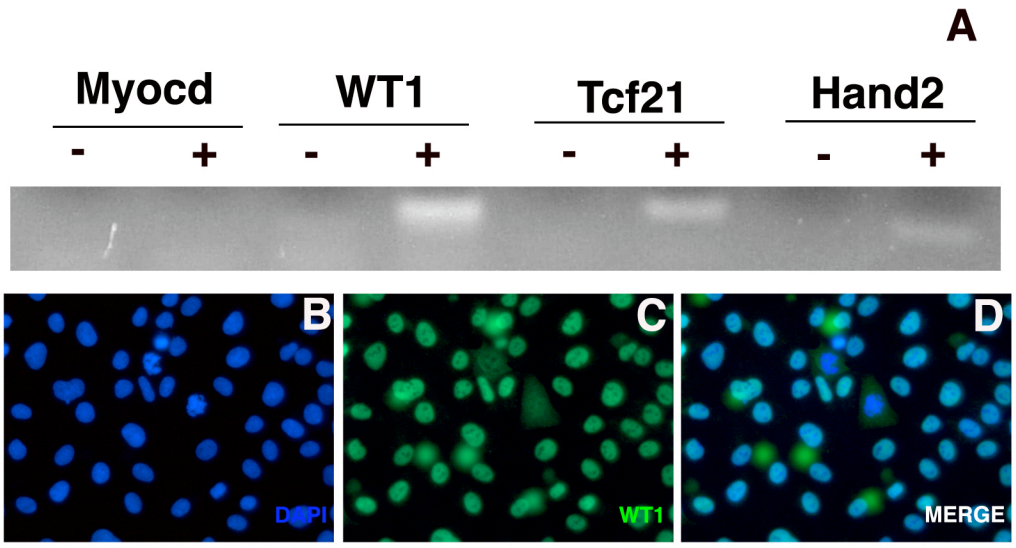

Figure 13: *Hand2* is expressed in epicardial cultures. RT-PCR on 4-day epicardial explants indicates *Hand2* is expressed in epicardial cultures (A). Imunocytochemistry indicates an enrichment for epicardial cells in the explant cultures (B-D).

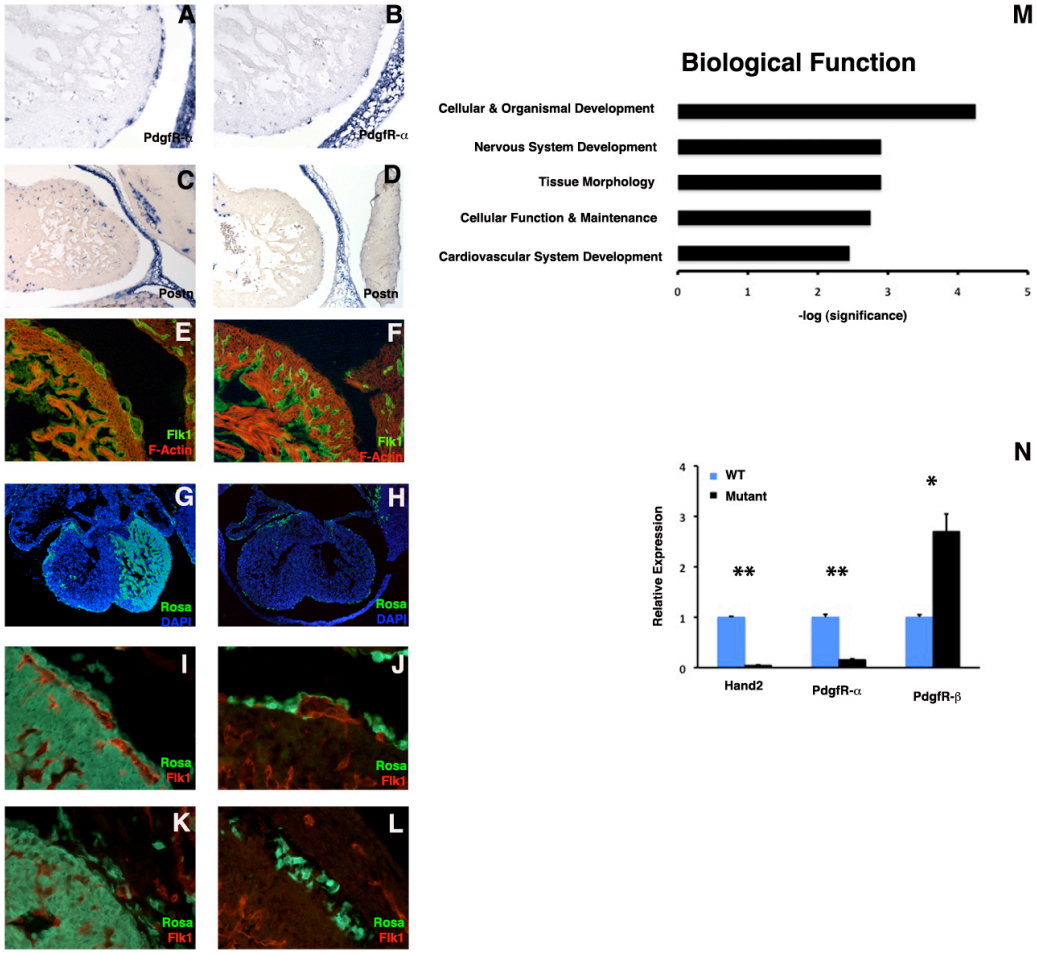

Figure 14: Fibroblast lineage and secondary coronary defects in *H2CKOs.* RNA *ISH* at E12.5 for *PDGFRα* and *Postn* (A-D). A decrease in fibroblasts is observed in the compact zone of *H2CKOs*. Immunohistochemistry for Flk1 (green) and F actin (red) at E12.5 (E-F). A decrease in coronary vasculature is observed in *H2CKOs*. Immunohistochemistry at E13.5 for the *Hand1* lineage (G) and the *Wt1* lineage (H) showing staining specificity in phenotypically wild-type mice. E13.5 *Hand1* lineage (G,I), *H2CKO* (K), *Wt1* lineage (H,J), and *Wt1*

conditional knockouts of *Hand2* (L). Immunohistochemistry for Flk1 (red) and Lineage (green) confirms coronary vessels are not derived from the epicardium, but *Hand2* conditional deletion in the epicardium leads to epicardial defects and absent coronary vessels. Gene ontology analysis microarray showing affected pathways in *H2CKO* isolated epicardium (M). qRTPCR on WT (blue bar) and *H2CKO* (black bar) isolated epicardium; n=4 (N). Asterisks indicate statistical significance: *$p < 0.05$; **$p < 0.01$.

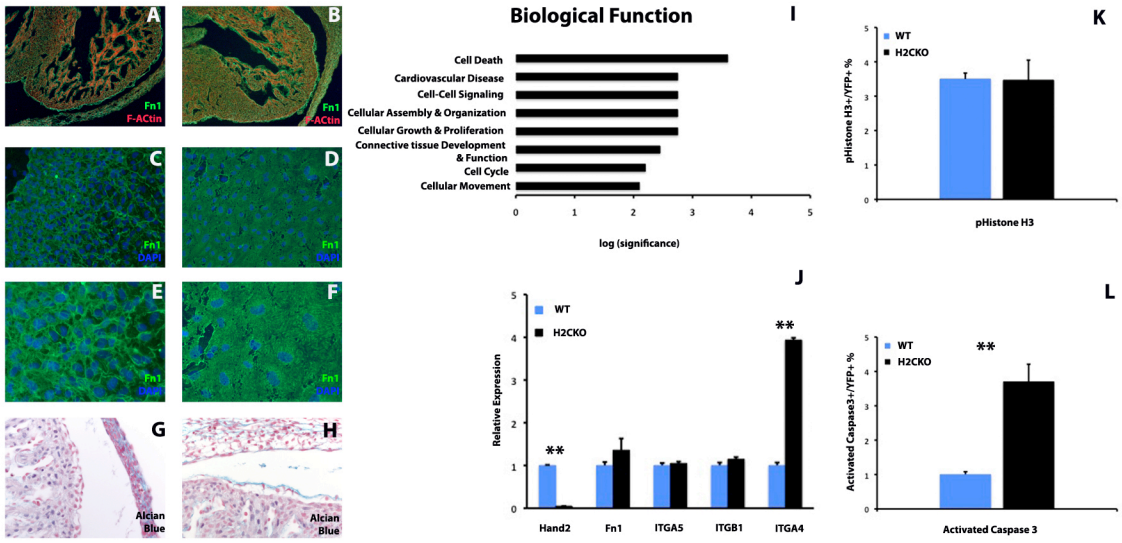

Figure 15: Abnormal Fn1 matrix assembly and function results in matrix related defects and impaired epicardial development. Immunohistochemistry at E12.5 for *Fn1* (green) and F-actin (red) showing Fn1 expression in the epicardium and displaying absent coronary vessels (A,B). Isolated epicardial cells show an aberration from normal Fn1 localization, where WT epicardial cells distribute Fn1 in a series of well formed lattices, Fn1 appears to be distributed uniformly throughout the cells, further suggesting migratory defects in *H2CKO* epicardial cells (C-F). An increase in alcian blue staining the epicardium indicates increased ECM (G,H). Gene ontology analysis microarray showing affected pathways in *H2CKO* isolated epicardium (I). qRTPCR on WT (blue bar) and *H2CKO* (black bar) isolated epicardium; n=4 (J). Cell proliferation (K) and Cell apoptosis (L) on WT and *H2CKO* embryos at E12.5; n=3. Asterisks indicate statistical significance: *$p < 0.05$; **$p < 0.01$.

Chapter Five

Methods

Targeting *Hand1* and Generation of Mice

To construct the targeting vector, a 3.4Kb EGFPCre cassette (kindly provided by Dr. Simon J. Conway) was isolated with a *XhoI*/*HindIII* digest and ligated into pBluescript SK+. A 3.0Kb *BstEII* fragment, cloned into pBluescript SK(+), upstream from the *Hand1* translational initiation codon was isolated with a *XhoI* digest and ligated 5' of the EGFPCre cassette. A 1.75Kb *Frt*-flanked neomycin cassette was isolated from ploxFlpneo (provided by Thomas Saunders U. Michigan) with an *EcoRI/NotI* digest and ligated 3' of the EGFPCre cassette. A 1.6Kb *SalI*/*HindIII* fragment, cloned into pBluescript SK(+), that extended from within the first intron of the gene into the second exon was isolated with a *NotI* digest and cloned 3' of the neomycin cassette. The targeting vector was linearized with *XhoI*, prior to electroporation into CCE 916 wildtype ES cells, and plated onto G418-resistant STO feeder layers. Following positive selection with G418, individual ES colonies were isolated and analyzed by Southern blot for homologous recombination at the *Hand1* locus, as previously described(Firulli et al., 1998). Homologous recombination was observed at a frequency of 1:4 in the 150 ES cell clones analyzed. Four independent clones were injected into blastocysts obtained from C57/B6 mice, which were subsequently implanted into pseudopregnant Swiss foster females. Chimeras that were obtained transmitted

the *Hand1* mutation through the germline and the resulting offspring were intercrossed with homozygous $R26^{Fki}$ (FLPeR) mice on a pure 129/SvJaeSor genetic background to permanently delete the neomycin cassette. Offspring were then intercrossed to remove the $R26^{Fki}$ allele.

Genotyping

ES cell DNA, as well as tail genomic DNA from $Hand1^{EGFPCre\Delta Neo/+}$ mice, were analyzed for the *Hand1* mutation by Southern-blot analysis(Firulli et al., 1998). Insertion of the *EGFPCre* and *neo* genes into the *Hand1* locus introduced an *EcoRI* site that could be used to distinguish the wild-type and targeted alleles, which yielded 10.0Kb and 4.0Kb fragments, respectively, following Southern analysis of *EcoRI*-digested DNA and hybridization with a labeled *BssHII-XhoI* probe from the region 3' of the targeted mutation. Following removal of the *neo* gene, the 4.0Kb fragment shifted to a 2.25Kb fragment. Since the targeting construct did not contain a negative selection gene, an 861bp *NcoI* fragment from the *EGFPCre* cassette was labeled and hybridized to *EcoRI*-digested DNA, yielding a 10.0Kb band. Ectopic bands were not detected.

ROSA26R homozygous mice were genotyped using a probe located 5' of the STOP Flox (provided by Dr. Phillippe Soriano). Southern analysis of *EcoRV*-digested DNA was hybridized with labeled probe and yielded a 3.8Kb band.

The *Wnt1-Cre* transgene was detected in genomic DNA isolated from tail samples using the primers 5'–TCGATGCAACGAGTGATGAG–3' and 5'–

TTCGGCTATACGTAACAGGG–3', which recognize the sequence encoding *Cre*, and generate a ~470bp amplicon.

The *Hand2*$^{flox/flox}$ mice and *Wt1*^{ERT2Cre} mice (provided by William Pu Harvard) were genotyped as previously described (Morikawa and Cserjesi, 2008; Zhou et al., 2008).

Mating Schemes and Histological Preparations

Hand1$^{EGFPCre\Delta Neo/+}$, *WT1*^{ERT2Cre} and *Wnt-Cre* males were crossed to *ROSA26R* reporter mice(Soriano, 1999). *Hand1*$^{EGFPCre\Delta Neo/+}$; *Hand2*$^{+/-}$ and *WT1*^{ERT2Cre}; *Hand2*$^{+/-}$ mice were crossed to *Hand2*$^{flox/flox}$*; ROSA26R* reporter mice (LacZ or eYFP) to generate conditional null *Hand2* embryos.

X-gal staining, and histological preparations were done as previously described for paraffin embedded sections and whole mounts(Vincentz et al., 2008). For E15.5 and adult heart, embryos/tissues were dissected in PBS and fixed in a 1:1 mixture of 4% paraformaldehyde (PFA) in phospho-buffered saline (PBS) and 1X PBS for 5 minutes at 4^{O}C. Samples were then moved to 30% sucrose in 1X PBS overnight at 4^{O}C. Samples were then cryoprotected and stored at -80^{O}C. Samples were sectioned at 10-20mm and washed for 5 minutes in 1X PBS. Sections were then post-fixed in 0.5% PFA for 2 minutes, rinsed in 1X PBS then washed in 1X PBS for 10 minutes. Slides were then incubated with X-gal solution in the dark at 37^{O}C overnight. Slides were rinsed in 1X PBS and then post-fixed in 4% PFA for 20 minutes and then were washed three times in

1X PBS at room temperature for 5 minutes each. Slides were counterstained with Nuclear Fast Red.

Section RNA *In Situ* Hybridization

Section *in situ* hybridization was performed essentially as previously described(Vincentz et al., 2008). Antisense digoxygenin-labeled riboprobes were transcribed with T7, T3, or SP6 (Roche) following linearization of template DNA.

Whole Mount RNA *In Situ* Hybridization

Whole mount *in situ* hybridization was performed essentially as previously described(Nagy, 2003). Antisense digoxygenin-labeled riboprobes were transcribed for *Hand1* and *Tbx5*. For double in situ hybridization modifications were made as previously described (Ishii et al., 2007). Briefly, a riboprobe for *Hand1* was detected using anti-digoxigenin antibody and NBT/BCIP substrate. After the removal of the antibody by incubating twice with glycine-HCl (pH 2.2), the *Mlc2A* probe was detected using anti-fluorescein antibody and INT/BCIP substrate. After color development was completed, embryos were fixed with 4% paraformaldehyde in phosphate-buffered saline (PBS).

Primary Epicardial Culture

Primary epicardial cultures were isolated and cultured as previously described for both *WT* and *H2CKO* (Rhee et al., 2009). E11.5 hearts were explanted for 48 hours before removal. Isolated epicardial cells were cultured for an additional 48 hours before RNA isolation or immunocytochemistry.

Immunocytochemistry

Primary epicardial cultures were fixed in 4% PFA for 10 minutes, washed, and incubated in 0.1% Sodium Borohydride for 30 minutes. Cells were permeabilized with 0.15% Trition, blocked with 2% normal serum, and incubated with primary antibodies for Fn1 (Abcam). Secondary antibodies were conjugated with Alexa 488 (Molecular Probes) and counter stained with DAPI.

Immunohistochemistry

Embryos were fixed in 4% PFA overnight then embedded in paraffin or cryoprotected and sectioned at 7mm. Antibody staining for α-SMA (Sigma), Tyrosine Hydroxylase, and Tubb3 (Abcam) was done as previously described on paraffin embedded samples (Snider et al., 2008). Frozen sections were washed in PBS, blocked in 1.5% normal serum for 30 minutes followed by a serum-free protein block (Dako) for 10 minutes. Primary antibody for Flk1 (Abcam), Fn1 (Abcam), pHistone H3 (Abcam), aactivated-Caspase 3 (Promega), α-SMA (Sigma), and GFP (Invitrogen) were incubated at $4^{O}C$ overnight. Secondary antibodies were conjugated with Alexa 488 or 594 (Molecular Probes). Alexa 594-conjugated Phalloidin was used to dye F-Actin filaments (Molecular Probes).

Whole Mount Immunohistochemistry

For whole-mount immunohistochemistry with Rat α-CD31 (BD Pharmingen, Cat# 550274), embryos were collected in 1X PBS and were fixed overnight in 4% PFA. Embryos were rinsed in 1X PBS three times and

dehydrated through a methanol gradient (25%, 50%, 75%, 100% twice), and stored at –20^{O}C until use. Embryos were bleached for 1 hour on ice in 5% H_2O_2/methanol. Embryos were then rinsed in 100% methanol for 10 minutes and rehydrated thru a methanol gradient. The remainder of steps were then carried out at 4' on a nutator. Embryos were washed three times in PBTXX (1X PBS, 1% Triton X-100) and then blocked in PBSMT (1X PBS, 2% nonfat instant skim milk, 0.5% Trition X-100) for 2 hours. The blocking solution was then removed and embryos were incubated overnight in PBSMT with 1' antibody (1:250). The following day, embryos were washed five times in PBSMT for 1 hour each. Embryos were then incubated in PBSMT with Goat α-RAT (ABCAM, Cat# AB7097) 2' antibody (1:250). The following day embryos were washed five times in PBSMT for 1 hour each. Embryos were then washed twice in PBTXX for 10 minutes at room temperature. Embryos were developed using DAB substrate kit (VECTOR, SK-4100).

Clearing of Embryos

Hand1$^{LacZ/+}$ mice, *Hand1*$^{EGFPCre\Delta Neo/+}$ mice, and PECAM immunohistochemistry stained embryos were cleared following dehydration washing embryos in BABB (Benzyl Benzoate:Benzyl Alcohol at a 2:1 concentration). Embryos were photographed with bright field illumination.

Quantitative RT-PCR

Total RNA was isolated from flash-frozen E12.5 hearts or primary epicardial cultures using the High Pure RNA Tissue or Isolation Kit (Roche). Total RNA served as a template to generate cDNA using the Transcriptor First Strand cDNA Synthesis Kit (Roche) or WGA1 Whole Genome Amplification Kit (Sigma). For quantitative real-time PCR, cDNA was amplified using Lightcycler 480 Probes Master (Roche). Target gene specific assays were were designed in accordance with the UPL probe library (Roche). Relative gene expression was determined by using standard curves and normalized to *GAPDH*. 3-6 samples were collected per assay. Differences between groups were examined for statistical significance using the Student's t-test. P values of <0.05 were regarded as significant.

References

Abe, M., Tamamura, Y., Yamagishi, H., Maeda, T., Kato, J., Tabata, M.J., Srivastava, D., Wakisaka, S., and Kurisu, K. (2002). Tooth-type specific expression of dhand/HAND2: possible involvement in murine lower incisor morphogenesis. Cell Tissue Res *310*, 201-212.

Abremski, K., and Hoess, R. (1992). Evidence For A Second Conserved Arginine Residue In The Integrase Family Of Recombination Proteins. Protein Engineering Design & Selection *5*.

Abremski, K., Hoess, R., and Sternberg, N. (1983). Studies On The Propertie of P1 Site-Specific Recombination: Evidence For Topologically Unlinked Products Following Recombination. Cell *32*, 1301-1311.

Abu-Issa, R., and Kirby, M.L. (2007). Heart field: from mesoderm to heart tube. Annual review of cell and developmental biology *23*, 45-68.

Ahn, K., Mishina, Y., Hanks, M.C., Behringer, R.R., and Crenshaw, E.B., 3rd (2001). BMPR-IA signaling is required for the formation of the apical ectodermal ridge and dorsal-ventral patterning of the limb. Development *128*, 4449-4461.

Armstrong, E.J., and Bischoff, J. (2004). Heart valve development: endothelial cell signaling and differentiation. Circulation research *95*, 459-470.

Barbosa, A.C., Funato, N., Chapman, S., McKee, M.D., Richardson, J.A., Olson, E.N., and Yanagisawa, H. (2007). Hand transcription factors cooperatively regulate development of the distal midline mesenchyme. Developmental biology *310*, 154-168.

Barnes, R.M., and Firulli, A.B. (2009). A Twist of insight, the role of Twist-Family bHLH factors in development. . Int J Dev Biol *53*, 909-924.

Bazigou, E., Xie, S., Chen, C., Weston, A., Miura, N., Sorokin, L., Adams, R., Muro, A.F., Sheppard, D., and Makinen, T. (2009). Integrin-alpha9 is required for fibronectin matrix assembly during lymphatic valve morphogenesis. Developmental cell *17*, 175-186.

Bruneau, B.G. (2002). Transcriptional regulation of vertebrate cardiac morphogenesis. Circulation research *90*, 509-519.

Cai, C.L., Liang, X.H., Shi, Y., Chu, P.H., Pfaff, S.L., Chen, J., and Evans, S. (2003). Isl1 identifies a cardiac progenitor population that proliferates prior to differentiation and contributes a majority of cells to the heart. Dev Cell *5*, 877-889.

Cai, C.L., Martin, J.C., Sun, Y., Cui, L., Wang, L., Ouyang, K., Yang, L., Bu, L., Liang, X., Zhang, X.*, et al.* (2008). A myocardial lineage derives from Tbx18 epicardial cells. Nature *454*, 104-108.

Chen, H., and Johnson, R.L. (2002). Interactions between dorsal-ventral patterning genes lmx1b, engrailed-1 and wnt-7a in the vertebrate limb. The International journal of developmental biology *46*, 937-941.

Chen, H., Lun, Y., Ovchinnikov, D., Kokubo, H., Oberg, K.C., Pepicelli, C.V., Gan, L., Lee, B., and Johnson, R.L. (1998). Limb and kidney defects in Lmx1b mutant mice suggest an involvement of LMX1B in human nail patella syndrome. Nature genetics *19*, 51-55.

Christoffels, V.M., Grieskamp, T., Norden, J., Mommersteeg, M.T., Rudat, C., and Kispert, A. (2009). Tbx18 and the fate of epicardial progenitors. Nature *458*, E8-9; discussion E9-10.

Cserjesi, P., Brown, D., Lyons, G.E., and Olson, E.N. (1995). Expression of the novel basic helix-loop-helix gene eHAND in neural crest derivatives and extra embryonic membranes during mouse development. Developmental biology *170*, 664-678.

Danielian, P.S., Muccino, D., Rowitch, D.H., Michael, S.K., and McMahon, A.P. (1998). Modification Of Gene Activity In Mouse Embryos *In Utero* By A Tamoxifen-Inducible Form Of Cre Recombinase. Current Biology *8*, 1323-1328.

Eisenberg, L.M., and Markwald, R.R. (1995). Molecular regulation of atrioventricular valvuloseptal morphogenesis. Circulation research *77*, 1-6.

Farley, F.W., Soriano, P., Steffen, L.S., and Dymecki, S.M. (2000). Widespread recombinase expression using FLPeR (flipper) mice. Genesis *28*, 106-110.

Fernandez-Teran, M., Piedra, M.E., Kathiriya, I.S., Srivastava, D., Rodriguez-Rey, J.C., and Ros, M.A. (2000). Role of dHAND in the anterior-posterior polarization of the limb bud: implications for the Sonic hedgehog pathway. Development *127*, 2133-2142.

Fernandez-Teran, M., Piedra, M.E., Rodriguez-Rey, J.C., Talamillo, A., and Ros, M.A. (2003). Expression and regulation of eHAND during limb development. Dev Dyn *226*, 690-701.

Firulli, A.B. (2003). A HANDful of questions: The molecular biology of the HAND-subclass of basic helix-loop-helix transcription factors. Gene *312C*, 27-40.

Firulli, A.B., McFadden, D.G., Lin, Q., Srivastava, D., and Olson, E.N. (1998). Heart and extra-embryonic mesodermal defects in mouse embryos lacking the bHLH transcription factor Hand1. Nature genetics *18*, 266-270.

Firulli, A.B., and Thattaliyath, B.D. (2002). Transcription factors in cardiogenesis: The combinations that may unlock the mysteries of the heart. Inter Rev Cytol *214*, 1-62.

Firulli, B.A., Krawchuk, D., Centonze, V.E., Virshup, D.E., Conway, S.J., Cserjesi, P., Laufer, E., and Firulli, A.B. (2005). Altered Twist1 and Hand2 dimerization is associated with Saethre-Chotzen syndrome and limb abnormalities. Nat Genet *37*, 373-381.

Firulli, B.A., Redick, B.A., Conway, S.J., and Firulli, A.B. (2007). Mutations within helix I of Twist1 result in distinct limb defects and variation of DNA binding affinities. The Journal of biological chemistry *282*, 27536-27546.

Frisch, S.M., and Francis, H. (1994). Disruption of epithelial cell-matrix interactions induces apoptosis. J Cell Biol *124*, 619-626.

George, E.L., Baldwin, H.S., and Hynes, R.O. (1997). Fibronectins are essential for heart and blood vessel morphogenesis but are dispensable for initial specification of precursor cells. Blood *90*, 3073-3081.

George, E.L., Georges-Labouesse, E.N., Patel-King, R.S., Rayburn, H., and Hynes, R.O. (1993). Defects in mesoderm, neural tube and vascular development in mouse embryos lacking fibronectin. Development *119*, 1079-1091.

Georges-Labouesse, E.N., George, E.L., Rayburn, H., and Hynes, R.O. (1996). Mesodermal development in mouse embryos mutant for fibronectin. Developmental Dynamics *207*, 145-156.

Grieshammer, U., Minowada, G., Pisenti, J.M., Abbott, U.K., and Martin, G.R. (1996). The chick limbless mutation causes abnormalities in limb bud dorsal-ventral patterning: implications for the mechanism of apical ridge formation. Development *122*, 3851-3861.

Guo, F., Gopaul, D., and van Duyne, G. (1997). Structure of Cre Recombinase Complexed With DNA In A Site-Specific Recombination Synapse. Nature *389*, 40-46.

Hamilton, D., and Abremski, K. (1984). Site-Specific Recombination By The bacteriophage P1 lox-Cre System. Cre-mediated synapsis of two lox site Journal of Molecular biology *178*, 481-486.

Hendershot, T.J., Liu, H., Clouthier, D.E., Shepherd, I.T., Coppola, E., Studer, M., Firulli, A.B., Pittman, D.L., and Howard, M.J. (2008). Conditional deletion of Hand2 reveals critical functions in neurogenesis and cell type-specific gene expression for development of neural crest-derived noradrenergic sympathetic ganglion neurons. Developmental biology.

Hiruma, T., Nakajima, Y., and Nakamura, H. (2002). Development of pharyngeal arch arteries in early mouse embryo. Journal of anatomy *201*, 15-29.

Hoess, R., and Abremski, K. (1985). Mechanism of Strand Cleavage and Exchange in the Cre-*lox* site-specific recombination system. Journal of Molecular Biology *181*, 351-362.

Hoess, R., Wierzbicki, A., and Abremski, K. (1986). The Role of The *loxP* Spacer Region in P1 Site-Specific Recombination. Nucleic Acids Research *14*, 2287-2300.

Hollenberg, S.M., Sternglanz, R., Cheng, P.F., and Weintraub, H. (1995). Identification of a new family of tissue-specific basic helix-loop-helix proteins with a two-hybrid system. Molecular and cellular biology *15*, 3813-3822.

Holler, K.L., Hendershot, T.J., Troy, S.E., Vincentz, J.W., Firulli, A.B., and Howard, M.J. (2010). Targeted deletion of Hand2 in cardiac neural crest-derived cells influences cardiac gene expression and outflow tract development. Developmental biology *341*, 291-304.

Ieda, M., Tsuchihashi, T., Ivey, K.N., Ross, R.S., Hong, T.T., Shaw, R.M., and Srivastava, D. (2009). Cardiac fibroblasts regulate myocardial proliferation through beta1 integrin signaling. Developmental cell *16*, 233-244.

Ikeda, H., and Tomizawa, J. (1968). Prophage P1, an Extrachromosomal Element. . Cold Spring Harbor Symp Quant Biol *33*, 791-798.

Ishii, Y., Langberg, J.D., Hurtado, R., Lee, S., and Mikawa, T. (2007). Induction of proepicardial marker gene expression by the liver bud. Development *134*, 3627-3637.

Jabs, E.W. (2004). TWIST and Saethre-Chotzen Syndrome. In Inborn errors of development, C.J. Epstein, R.P. Erickson, and A. Wynshaw-Boris, eds. (New York, Oxford University Press), pp. 401-409.

Johnson, R.L., and Tabin, C.J. (1997). Molecular models for vertebrate limb development. Cell *90*, 979-990.

Kadler, K.E., Hill, A., and Canty-Laird, E.G. (2008). Collagen fibrillogenesis: fibronectin, integrins, and minor collagens as organizers and nucleators. Current opinion in cell biology *20*, 495-501.

Kelly, R.G. (2005). Molecular inroads into the anterior heart field. Trends in cardiovascular medicine *15*, 51-56.

Kirby, M.L. (2007). Cardiac development (Oxford ; New York, Oxford University Press).

Kreuger, J., Jemth, P., Sanders-Lindberg, E., Eliahu, L., Ron, D., Basilico, C., Salmivirta, M., and Lindahl, U. (2005). Fibroblast growth factors share binding sites in heparan sulphate. Biochemical Journal *389*, 145-150.

Landy, A. (1993). Mechanistic and Structural Complexity in The Site-Specific Recombination Pathways of Int & Flp. Current Opinions In Genetics & Developent *3*, 699-707.

Lasko, M., Sauer, B., Mosinger, B., Lee, E., Manning, R., Yu, S.-H., Mulder, K., and Westphal, H. (1992). Targeted Oncogene Activation By Site-Specific Recombination In Transgenic Mice. Proceedings Of The National Academy Of Science *89*, 6232-6236.

Leiss, M., Beckmann, K., Giros, A., Costell, M., and Fassler, R. (2008). The role of integrin binding sites in fibronectin matrix assembly in vivo. Current opinion in cell biology *20*, 502-507.

Liao, Y.F., Gotwals, P.J., Koteliansky, V.E., Sheppard, D., and Van De Water, L. (2002). The EIIIA segment of fibronectin is a ligand for integrins alpha 9beta 1 and alpha 4beta 1 providing a novel mechanism for regulating cell adhesion by alternative splicing. The Journal of biological chemistry *277*, 14467-14474.

Massari, M.E., and Murre, C. (2000). Helix-loop-helix proteins: regulators of transcription in eucaryotic organisms. Molecular and cellular biology *20*, 429-440.
McFadden, D.G., Barbosa, A.C., Richardson, J.A., Schneider, M.D., Srivastava, D., and Olson, E.N. (2005). The Hand1 and Hand2 transcription factors regulate expansion of the embryonic cardiac ventricles in a gene dosage-dependent manner. Development *132*, 189-201.

McFadden, D.G., Charite, J., Richardson, J.A., Srivastava, D., Firulli, A.B., and Olson, E.N. (2000). A GATA-dependent right ventricular enhancer controls dHAND transcription in the developing heart. Development *127*, 5331-5341.

McFadden, D.G., McAnally, J., Richardson, J.A., Charite', J., and Olson, E.N. (2002). Misexpression of dHAND induces ectopic digits in the developing limb bud in the absence of direct DNA binding. Development *129*, 3077-3088.

Mellgren, A.M., Smith, C.L., Olsen, G.S., Eskiocak, B., Zhou, B., Kazi, M.N., Ruiz, F.R., Pu, W.T., and Tallquist, M.D. (2008). Platelet-derived growth factor receptor beta signaling is required for efficient epicardial cell migration and development of two distinct coronary vascular smooth muscle cell populations. Circulation research *103*, 1393-1401.

Moore, A.W., McInnes, L., Kreidberg, J., Hastie, N.D., and Schedl, A. (1999). YAC complementation shows a requirement for Wt1 in the development of epicardium, adrenal gland and throughout nephrogenesis. Development *126*, 1845-1857.

Morikawa, Y., and Cserjesi, P. (2004). Extra-embryonic vasculature development is regulated by the transcription factor HAND1. Development *131*, 2195-2204.

Morikawa, Y., and Cserjesi, P. (2008). Cardiac neural crest expression of Hand2 regulates outflow and second heart field development. Circulation research *103*, 1422-1429.

Morikawa, Y., D'Autreaux, F., Gershon, M.D., and Cserjesi, P. (2007). Hand2 determines the noradrenergic phenotype in the mouse sympathetic nervous system. Developmental biology *307*, 114-126.

Nagy, A. (2000). Cre Recombinase: The Universal Reagent for Genome Tailoring. Genesis *26*, 99-109.

Nagy, A. (2003). Manipulating the mouse embryo : a laboratory manual, 3rd edn (Cold Spring Harbor, N.Y., Cold Spring Harbor Laboratory Press).

Olson, E.N. (2002). A genetic blueprint for growth and development of the heart. Harvey Lectures *98*, 41-64.

Red-Horse, K., Ueno, H., Weissman, I.L., and Krasnow, M.A. (2010). Coronary arteries form by developmental reprogramming of venous cells. Nature *464*, 549-553.

Rhee, D.Y., Zhao, X.Q., Francis, R.J., Huang, G.Y., Mably, J.D., and Lo, C.W. (2009). Connexin 43 regulates epicardial cell polarity and migration in coronary vascular development. Development *136*, 3185-3193.

Richarte, A.M., Mead, H.B., and Tallquist, M.D. (2007). Cooperation between the PDGF receptors in cardiac neural crest cell migration. Developmental biology *306*, 785-796.

Riley, P., Anson-Cartwright, L., and Cross, J.C. (1998). The Hand1 bHLH transcription factor is essential for placentation and cardiac morphogenesis. Nature genetics *18*, 271-275.

Rossant, J., and McMahon, A. (1999). "Cre"-ating Mouse Mutants - A Meeting Review On Conditional Mouse genetics. Genes & Development *13*, 142-145.

Sauer, B., and Henderson, N. (1988). Site-Specific DNA Recombination In Mammalian Cells By The Cre Recombinase of Bacteriophage P1. Proceedings Of The National Academy Of Science *85*, 5166-5170.

Shalaby, F., Rossant, J., Yamaguchi, T.P., Gertsenstein, M., Wu, X.F., Breitman, M.L., and Schuh, A.C. (1995). Failure of blood-island formation and vasculogenesis in Flk-1-deficient mice. Nature *376*, 62-66.

Snider, P., Hinton, R.B., Moreno-Rodriguez, R.A., Wang, J., Rogers, R., Lindsley, A., Li, F., Ingram, D.A., Menick, D., Field, L.*, et al.* (2008). Periostin is required for maturation and extracellular matrix stabilization of noncardiomyocyte lineages of the heart. Circulation research *102*, 752-760.

Soriano, P. (1999). Generalized lacZ Expression With The ROSA26 Cre Reporter Strain. Nature genetics *21*, 70-71.

Sottile, J., Hocking, D.C., and Swiatek, P.J. (1998). Fibronectin matrix assembly enhances adhesion-dependent cell growth. Journal of cell science *111 (Pt 19)*, 2933-2943.

Srivastava, D., Cserjesi, P., and Olson, E.N. (1995). A subclass of bHLH proteins required for cardiac morphogenesis. Science *270*, 1995-1999.

Srivastava, D., Thomas, T., Lin, Q., Kirby, M.L., Brown, D., and Olson, E.N. (1997). Regulation of cardiac mesodermal and neural crest development by the bHLH transcription factor, dHAND. Nature genetics *16*, 154-160.

Sternberg, N., and Hamilton, D. (1981). Bacteriophage P1 Site-Specific Recombination I. Recombination between *loxP* Sites. Journal of Molecular Biology *150*, 467-487.

Takeuchi, J.K., and Bruneau, B.G. (2009). Directed transdifferentiation of mouse mesoderm to heart tissue by defined factors. Nature.

Tallquist, M., and Kazlauskas, A. (2004). PDGF signaling in cells and mice. Cytokine Growth Factor Rev *15*, 205-213.

Tallquist, M.D., and Soriano, P. (2003). Cell autonomous requirement for PDGFRalpha in populations of cranial and cardiac neural crest cells. Development *130*, 507-518.

Thomas, T., Kurihara, H., Yamagishi, H., Kurihara, Y., Yazaki, Y., Olson, E.N., and Srivastava, D. (1998). A signaling cascade involving endothelin-1, dHAND and msx1 regulates development of neural-crest-derived branchial arch mesenchyme. Development *125*, 3005-3014.

Tomita, M., Okuyama, T., Katsuyama, H., Miura, Y., Nishimura, Y., Hidaka, K., Otsuki, T., and Ishikawa, T. (2007). Mouse model of paraquat-poisoned lungs and its gene expression profile. Toxicology *231*, 200-209.

Trinh, L.A., Yelon, D., and Stainier, D.Y. (2005). Hand2 regulates epithelial formation during myocardial diferentiation. Curr Biol *15*, 441-446.

Vincentz, J.W., Barnes, R.M., Rodgers, R., Firulli, B.A., Conway, S.J., and Firulli, A.B. (2008). An absence of Twist1 results in aberrant cardiac neural crest morphogenesis. Developmental biology.

Watt, A.J., Battle, M.A., Li, J., and Duncan, S.A. (2004). GATA4 is essential for formation of the proepicardium and regulates cardiogenesis. Proceedings of the National Academy of Sciences of the United States of America *101*, 12573-12578.

Wu, M., Smith, C.L., Hall, J.A., Lee, I., Luby-Phelps, K., and Tallquist, M.D. (2010). Epicardial spindle orientation controls cell entry into the myocardium. Developmental cell *19*, 114-125.

Yanagisawa, H., Clouthier, D.E., Richardson, J.A., Charite, J., and Olson, E.N. (2003). Targeted deletion of a branchial arch-specific enhancer reveals a role of dHAND in craniofacial development. Development *130*, 1069-1078.

Yang, J.T., Rayburn, H., and Hynes, R.O. (1995). Cell adhesion events mediated by alpha 4 integrins are essential in placental and cardiac development. Development *121*, 549-560.

Yin, C., Kikuchi, K., Hochgreb, T., Poss, K.D., and Stainier, D.Y. (2010). Hand2 regulates extracellular matrix remodeling essential for gut-looping morphogenesis in zebrafish. Developmental cell *18*, 973-984.

Yoziyanov, Y., Pathania, S., and Jayaram, M. (1999). A General Model For Site-Specific Recombination By The Integrase Family Recombinases. Nucleic Acids Research *27*, 930-941.

Zhou, B., Ma, Q., Rajagopal, S., Wu, S.M., Domian, I., Rivera-Feliciano, J., Jiang, D., von Gise, A., Ikeda, S., Chien, K.R.*, et al.* (2008). Epicardial progenitors contribute to the cardiomyocyte lineage in the developing heart. Nature *454*, 109-113.

CURRICULUM VITAE

Ralston M. Barnes

Education

2010	Ph.D.	**Indiana University**	Anatomy & Cell Biology
2002	M.S.	**Tulane University**	Cell & Molecular Biology
2001	B.A.	**Lehigh University**	Psychobiology
	Minor		Health and Human Development

Awards & Fellowships

2010 Chancelor's Scholar, Graduate School, Doctoral Program, IUPUI

7/08-7/10 Predoctoral Fellowship, American Heart Association (AHA): Lineage Analysis and Functional Redundancy of Hand Factors

Research & Training Experience

Positions

4/06-5/09 **Graduate Research Assistant in the laboratory of Dr. Anthony B. Firulli,** Department of Pediatrics, Wells Center for Pediatric Research, James Whitcomb Riley Hospital for Children, Indiana University School of Medicine Cancer Research Institute

1/02-1/06 **Graduate Research Assistant in the laboratory of Dr. Peter Cserjesi,** Department of Cell & Molecular Biology, Tulane University

Tutorials

12/01-8/02 Laboratory of Dr. Yiping Chen, Department of Cell & Molecular Biology, Tulane University

Publications:

1) **Barnes RM**, Firulli BA, Vincentz JW, Cserjesi P, Conway SJ, Firulli AB. Hand2 loss-of-function in Hand1-expressing cells Reveals Distinct Roles in Heart and Epicardial Development. *JCI* (In Preparation).
2) **Barnes RM**, Firulli BA, Conway SJ, Vincentz JW, Firulli AB. Analysis of the Hand1 Cell Lineage Reveals Novel Contributions to Cardiovascular,

Neural Crest, Extra-Embryonic, and Lateral Mesoderm Derivatives. *Dev Dyn*. (In Review).

3) Firulli BA, McConville DP, Vincentz JW, **Barnes RM**, Firulli AB. Analysis of a Hand1 hypomorphic allele reveals a critical threshold for embryonic viability. *Dev Dyn*. 2010.
4) Olaopa M, Caldwell RL, **Barnes RM**. Riley Heart Center Symposium on cardiac development 2009: transcriptional unification of heart morphogenesis. *Pediatric Cardiology* 2010.
5) **Barnes RM** & Firulli AB. A Twist of insight, the role of Twist-family bHLH factors in development. *International Journal of Developmental Biology* 2009.
6) Vincentz JW, **Barnes RM**, Firulli BA, Conway SJ, Firulli AB. Cooperative interaction of Nkx2.5 and Mef2c transcription factors during heart development. *Dev Dyn.* 2008.
7) Vincentz JW, **Barnes RM**, Rodgers R, Firulli BA, Conway SJ, Firulli AB. An absence of Twist1 results in aberrant cardiac neural crest morphogenesis. *Dev Biol*. 2008.

Professional Experience:

Conferences:

9/10	Poster Presentation, 34th Annual Midwest Pediatric Cardiology Society Scientific Session, Indianapolis, IN
5/10	Platform Presentation, 17th International Weinstein Cardiovascular Development Conference, Amsterdam, The Netherlands
5/09	Presentation of Platform Session, 16th International Weinstein Cardiovascular Development Conference, San Francisco, CA
5/08	Attended 15th International Weinstein Cardiovascular Development Conference, Houston, TX
5/07	Attended 14th International Weinstein Cardiovascular Development Conference, Indianapolis, IN
4/06	Platform Presentation, Developmental Biology Consortium, New Orleans, LA
4/05	Platform Presentation, Developmental Biology Consortium, New Orleans, LA
10/04	Attended, Southwest Regional Meeting of Developmental Biology, Dallas, TX